AD-A061 912 VOUGHT CORP ADVANCED TECHNOLOGY CENTER INC DALLAS TEX F/G 11/4
THE EFFECT OF ENVIRONMENT ON THE MECHANICAL BEHAVIOR OF AS/3501--ETC(U)
AUG 78 W J RENTON, T HO N00019-77-C-0369
UNCLASSIFIED ATC-B-92100/8CR-105 NL

| OF |
AD A061912

END
DATE FILMED
2 79
DDC

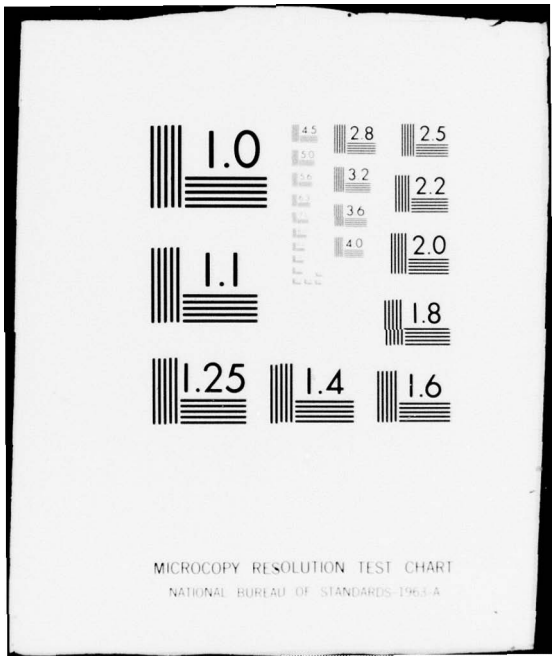
1.0
1.1
1.25
1.4
1.6
1.8
2.0
2.2
2.5
2.8
3.2
3.6
4.0
4.5
5.0
MICROCOPY RESOLUTION TEST CHART
NATIONAL BUREAU OF STANDARDS-1963-A

AD A061912

DDC FILE COPY

ATC Report No. B-92100/8CR-105

Contract No. N00019-77-C-0369

LEVEL II

THE EFFECT OF ENVIROMENT ON THE MECHANICAL BEHAVIOR OF AS/3501-6 GRAPHITE/EPOXY MATERIAL

W. J. Renton
T. Ho

Vought Corporation Advanced Technology Center
Dallas, Texas 75266

DDC
RECEIVED
DEC 7 1978
A

August 1978

Final Report for Period June 1977 - June 1978

Approved for public release; distribution unlimited

Prepared For:

Department of the Navy
Naval Air Systems Command
Washington, D.C. 20361

VOUGHT CORPORATION
advanced technology center, inc.

78 12 06 007

Unclassified

SECURITY CLASSIFICATION OF THIS PAGE *(When Data Entered)*

REPORT DOCUMENTATION PAGE

READ INSTRUCTIONS BEFORE COMPLETING FORM

1. REPORT NUMBER

2. GOVT ACCESSION NO.

3. RECIPIENT'S CATALOG NUMBER

4. TITLE *(and Subtitle)*

THE EFFECT OF ENVIRONMENT ON THE MECHANICAL BEHAVIOR OF AS/3501-6 GRAPHITE/EPOXY MATERIAL.

5. TYPE OF REPORT & PERIOD COVERED

FINAL REPORT FOR PERIOD JUNE 1977 - JUNE 1978

6. PERFORMING ORG. REPORT NUMBER

ATC [illegible]-B-92100/8CR-105

7. AUTHOR(s)

W. J. RENTON
T. HO

8. CONTRACT OR GRANT NUMBER(s)

N00019-77-C-0369

9. PERFORMING ORGANIZATION NAME AND ADDRESS

VOUGHT CORPORATION ADVANCED TECHNOLOGY CENTER, INC.
P. O. BOX 226144
DALLAS, TEXAS 75226

10. PROGRAM ELEMENT, PROJECT, TASK AREA & WORK UNIT NUMBERS

11. CONTROLLING OFFICE NAME AND ADDRESS

DEPARTMENT OF THE NAVY
NAVAL AIR SYSTEMS COMMAND
WASHINGTON, D.C. 20361

12. REPORT DATE

AUGUST 1978

13. NUMBER OF PAGES

74p.

14. MONITORING AGENCY NAME & ADDRESS *(if different from Controlling Office)*

15. SECURITY CLASS. *(of this report)*

UNCLASSIFIED

15a. DECLASSIFICATION/DOWNGRADING SCHEDULE

16. DISTRIBUTION STATEMENT *(of this Report)*

APPROVED FOR PUBLIC RELEASE: DISTRIBUTION UNLIMITED

17. DISTRIBUTION STATEMENT *(of the abstract entered in Block 20, if different from Report)*

18. SUPPLEMENTARY NOTES

19. KEY WORDS *(Continue on reverse side if necessary and identify by block number)*

COMPOSITE, TEMPERATURE, HUMIDITY, VISCOELASTICITY, EXTENSOMETER, CREEP, FATIGUE

20. ABSTRACT *(Continue on reverse side if necessary and identify by block number)*

Applicability of linear viscoelasticity to the characterization of AS/3501-6 Gr/Ep material under severe environment was investigated in this Phase I program. Specific studies included development of master curves reflecting material dependence on time, temperature and humidity and resolution of the question as to whether a specific thermal conditioning environment can be directly substituted for a specific moisture conditioning environment over a prescribed temperature vs. humidity range. Moreover, the

DD FORM 1 JAN 73 1473 EDITION OF 1 NOV 65 IS OBSOLETE
S/N 0102-014-6601 |

Unclassified

SECURITY CLASSIFICATION OF THIS PAGE *(When Data Entered)*

389 797

gathering of initial fatigue test data was begun which will be used to ascertain the feasibility of predicting fatigue failure of a composite material by accounting for the linear viscoelastic behavior of the resin in various environments during Phase II.

Characterization of the composite was attained through its lamina creep compliances. The test technique was considered critical in the combined temperature and humidity environment. Both a coated strain gage concept and an extensometer technique were evaluated in order to obtain reliable displacement/strain readings from moisture saturated specimens that were tested at various temperature/humidity environments. Current results indicate that the extensometer is a more reliable technique for recording creep-recovery test data and low frequency fatigue test results. Specimens with 0°, 90° and ±45° layup were used for creep-recovery tests in various environments. Test data were analyzed by using a linear viscoelasticity theory and power law representation of creep compliance.

Because of the difficulty in getting Poisson's ratio through extensometer or strain gage techniques, an analytical procedure was developed to obtain shear compliance. Thus, the need to make lateral strain measurement for the determination of the pure shear properties was avoided. A test-analysis procedure was developed to generate the principal compliances S_{ij} and master curves for all environments based on minimal test results.

A structural application of the effect of environment on the skin/spar joint design was presented. NASTRAN analysis indicated that environment has a dramatic effect on the critical stress location of the joint design and provided guidelines for improved design.

FOREWORD

The study reported in this Phase I program entitled "The Effect of Environment on Mechanical Behavior of AS/3501-6 Graphite/Epoxy Material" was conducted by Vought Corporation Advanced Technology Center and was sponsored by the Naval Air Systems Command under Contract Number N00019-77-C-0369.

Mr. M. Stander was the Navy Project Manager and Dr. W. J. Renton was the Vought Program Manager. Other key personnel are Dr. T. Ho, Principal Investigator, Dr. D. H. Petersen, Technical Coordinator, and Dr. R. A. Schapery, Technical Consultant.

This study was conducted from June 1977 through June 1978.

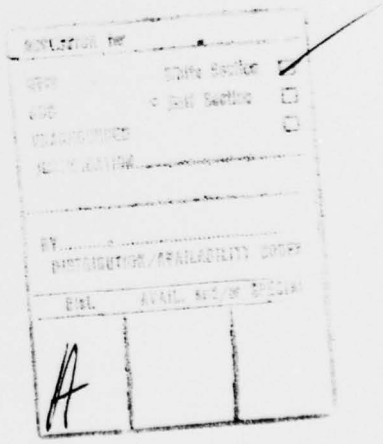

TABLE OF CONTENTS

TABLE OF CONTENTS
(Continued)

LIST OF FIGURES

LIST OF FIGURES
(Continued)

LIST OF TABLES

1.0 INTRODUCTION

Wide usage of advanced composite materials in aerospace systems is projected to become a reality over the next ten years. A V/STOL fighter aircraft is one of several Navy articles projected to be increasingly dependent on composite materials for primary and secondary structural components.

Presently, the response of advanced composite materials to arbitrary load and environments is known to have a significant adverse effect on the materials performance. The materials response in severe environments and related fatigue lifetime prediction methods are presently insufficient. This composites research program will assist in resolving this deficiency in the technology base. This in turn will ensure that the confident usage of advanced composite materials by the stress analyst and designer can be attained in the near future.

The overall objectives of this research program are:

- To ascertain if the mechanical response of AS/3501-6 graphite/epoxy composite material, subject to various time, temperature and moisture effects, can be characterized using traditional viscoelastic shift factors, and to formulate a master curve of material property dependence on time, temperature and humidity.
- To ascertain the feasibility of predicting fatigue failure of a composite material by accounting for the linear viscoelastic behavior of the resin in various temperature and humidity environments.
- To determine if a specific thermal conditioning environment can be directly substituted for a specific moisture conditioning environment, over a prescribed temperature vs. humidity range for AS/3501-6 graphite/epoxy material, and obtain an equivalent moisture effect on mechanical and fatigue properties. If this can be shown, a substantial cost and time savings in moisture conditioning of the test specimen can be achieved and possibly extended to other composite specimens.

This report covers a 12 month exploratory development program of the proposed research. AS/3501-6 Gr/Ep composite under severe environment was investigated. Application of linear viscoelasticity to characterize the mechanical response of the composite, subject to various time, temperature and moisture effects, was quite successful. We were able to formulate the master curves of material property and their dependence on time, temperature and humidity through test and analysis correlation. Also, a specific moisture environment is shown to be equivalent to a specific thermal conditioning environment through the shift factor from viscoelasticity theory where the temperature-shift factor and humidity-shift factor are additive in logarithmic scale.

A probabilistic study on fatigue failure prediction will be pursued in the Phase II program.

2.0 SPECIMEN FABRICATION

2.1 SPECIMEN FABRICATION

Hercules AS/3501-6 prepreg graphite/epoxy material was used in this program. It has a vendor suggested high service temperature capability and is under consideration for wide usage in Navy aircraft.

Fabrication of two composite panels was performed by Vought's manufacturing research and development division per the fabrication procedures recommended by Hercules. One composite panel was of unidirectional (0°) fiber orientation, 15" x 76" x 0.10" (twenty plies). The second panel had a ± 45° fiber orientation, symmetric layup and was 14.0" x 37.0" x 0.10". Both panels were autoclave cured. Each had a process control specimen 3" x 16" x (16 plies thick) cured during the autoclave run. Prior to this, a quality control specimen was fabricated to check material quality and the fabrication process. Test of flexural strength and modulus, short beam shear strength and the fiber volume were performed on the quality control/specimen. Each test panel was inspected using ultrasonic C-scan to insure that all test specimens would be free of void inclusions.

The layup and cure procedures followed by Vought personnel for each laminate were:

- o Clean all tooling
- o Apply a mold release agent to the tooling
- o Cover both surfaces of the layup with peel ply
- o Cover both surfaces of the layup with TX-1040
- o Position the layup on the tool
- o Appiy the cork dam and 6 bleeder plies
- o Cover the layup with nylon film
- o Cover the layup with two plies of fiberglass bleeder cloth
- o Install the layup in a vacuum bag and place in an autoclave

and the cure cycle was:

- o Apply 25" Hg minimum vacuum
- o Apply 10 psi autoclave pressure

- o Heat to 350 ± 5°F applying 90 ± 5 psi autoclave pressure once the panel has reached 275 ± 5°F (DO NOT VENT)
- o Maintain the laminate at 350 ± 5°F for 120 ± 5 minutes
- o Cool slowly to below 160°F (Cool no faster than 5°F per minute - Cool down should take approximately 45 minutes) and release pressure
- o Post cure in an oven for 2 hours at 400 ± 5°F.

Mechanical property test results for both the process control panels and the quality control panels are summarized in Table 1. Both panels were of 0° fiber orientation. The short beam shear specimens had nominal dimensions 0.60" in length by 0.249" wide by 0.078" thick. The flexure specimens had nominal dimensions 2.43" in length by 0.500" wide by 0.077" thick. All specimens were tested at ambient conditions and loaded at 0.050 inches/minute. Inspection of Table 1 shows that the test results compare favorably to the vendors published values for this material.

The two composite panels were cut into test specimens with dimensions 6.5" x .75" x .1". This 0.75" width is to guard against the extension of the edge effect into the interior of the test specimens when high levels of moisture and temperature are present. End tabs were fiberglass/epoxy material of dimensions 1.0" long x 0.75" wide x 0.08" thick. A typical test specimen is shown in Figure 1.

2.2 MOISTURE ABSORPTION STUDY

Specimens for this program were required to be conditioned until they attained moisture equilibrium in the same environment that will be used for mechanical testing. To provide guideline data for the specimen conditioning, ten samples with dimensions 1.0" x 1.0"x 0.10" (five 90° samples and five ± 45° samples) were exposed in a 200°F and 95% R.H. chamber for moisture absorption testing. Several samples were covered with protective coating M-coat C or M-coat C and D (from Micro-Measurements) to study their effects on the sample's moisture absorption rate and maximum moisture absorption by weight. Samples were taken out for weighing regularly on a Mettler micro-balance.

The moisture absorption data for these samples are shown in Figures 2 through 5. The weight reduction shown for the "M-coat C" and the "M-coat C and D" curves in the initial segment of the moisture absorption vs. time curves is believed to be caused by incomplete cure of the coating. From these test curves it is apparent that the coating systems have reduced the maximum moisture content of the

TABLE 1. QUALITY ASSURANCE TEST DATA FOR AS/3501-6 GRAPHITE/EPOXY LAMINATES.

PANEL	SHORT BEAM SHEAR STRENGTH @ R.T. (PSI)	FLEXURAL STRENGTH @ R.T. (PSI)	FLEXURAL MODULUS @ R.T (PSI) X 10^6	AVERAGE FIBER VOLUME (%)
Quality Control	21,352	245,531	23.43	65.9
	21,674	201,889	20.72	
	21,418	225,755	21.30	
	Avg. 21,481	Avg. 224,391	Avg. 21.82	
Process Control	20,829	253,000	19.1	
	20,227	235,160	22.2	
	21,307	270,747	20.4	
	Avg. 20,787(17,500)	Avg. 252, 969(260,000)	Avg. 20.6(17.5)	

*Vendor Data Are in Parentheses for a 62% Fiber Volume per AS/3501-6 Data Sheet.

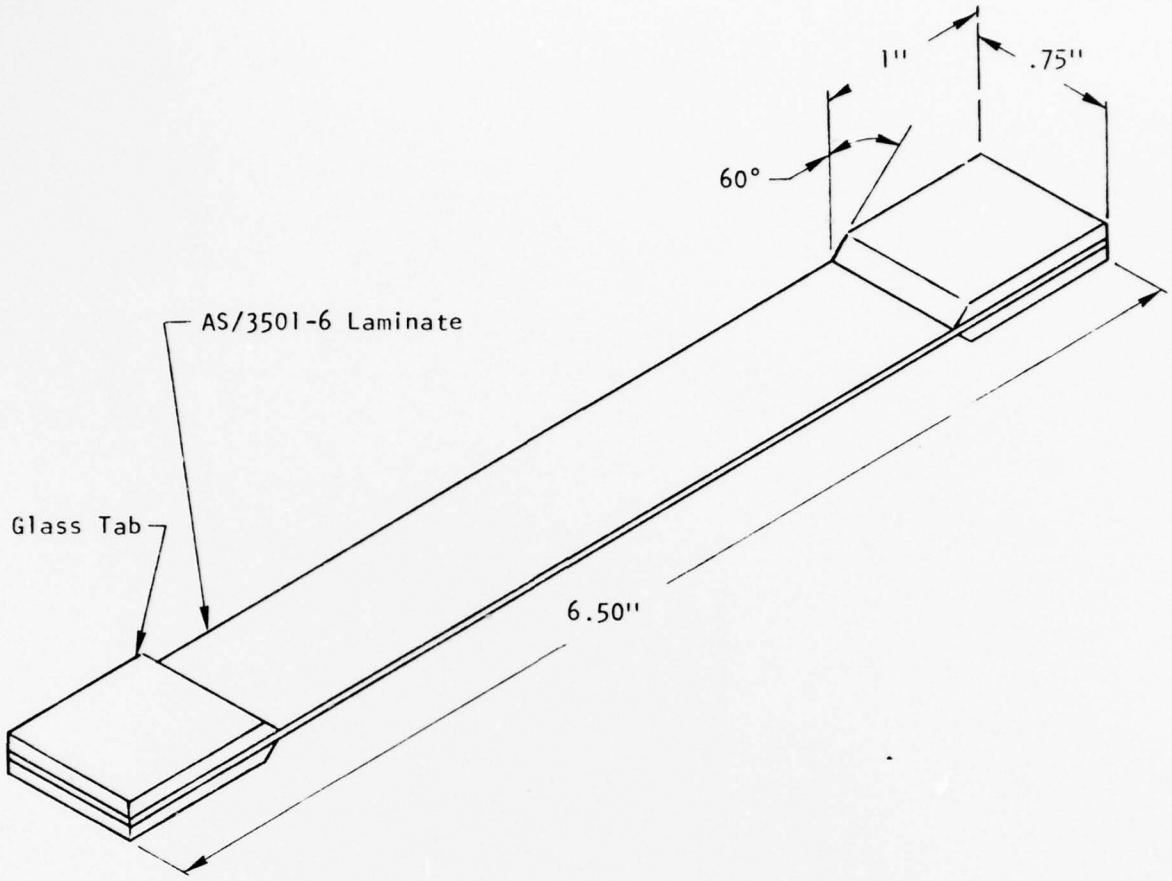

FIGURE 1. TYPICAL TEST SPECIMEN GEOMETRY.

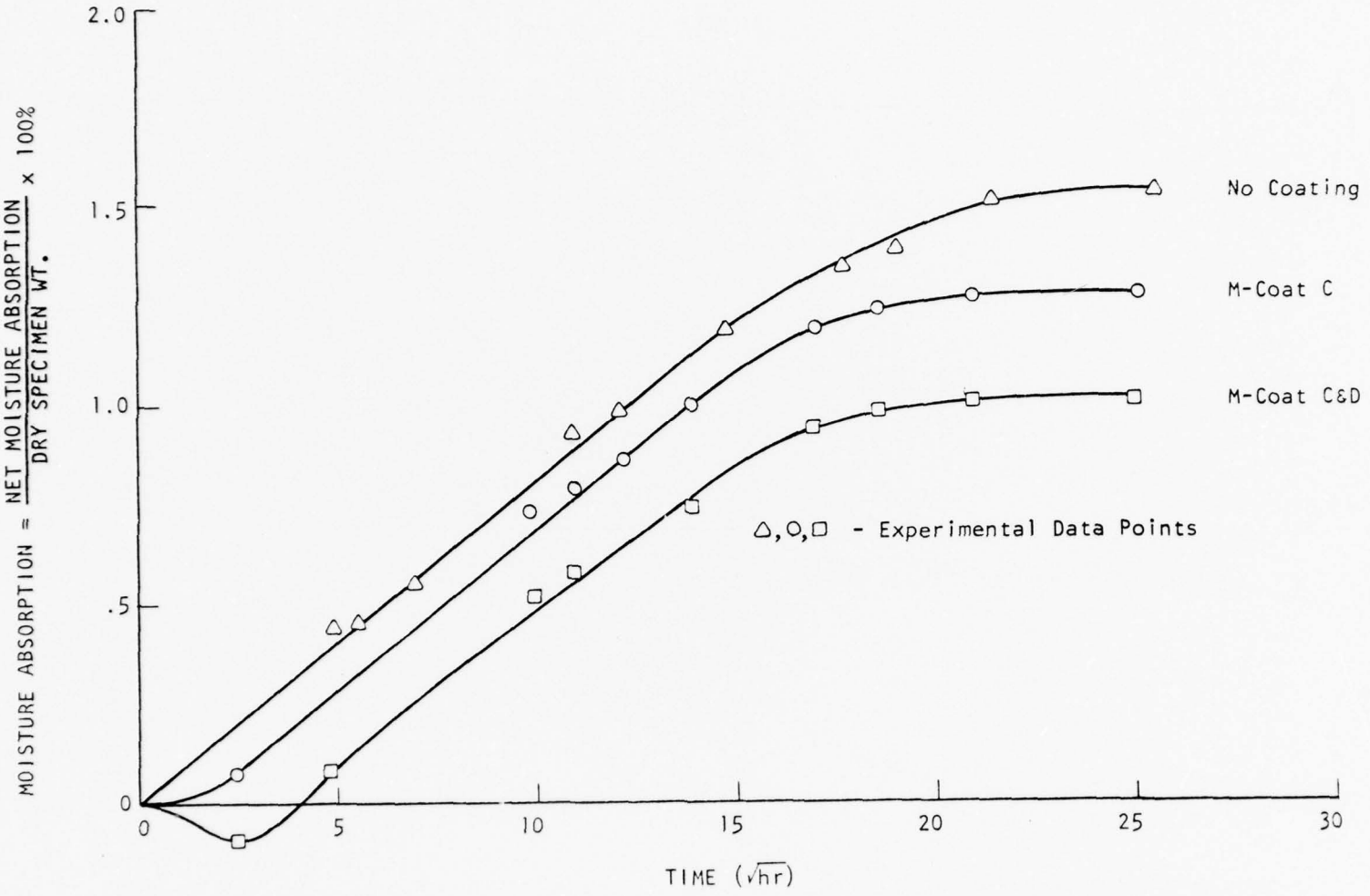

FIGURE 2. PERCENTAGE OF MOISTURE ABSORPTION OF ±45° GR/EP SPECIMEN UNDER 200°F AND 95% R.H.

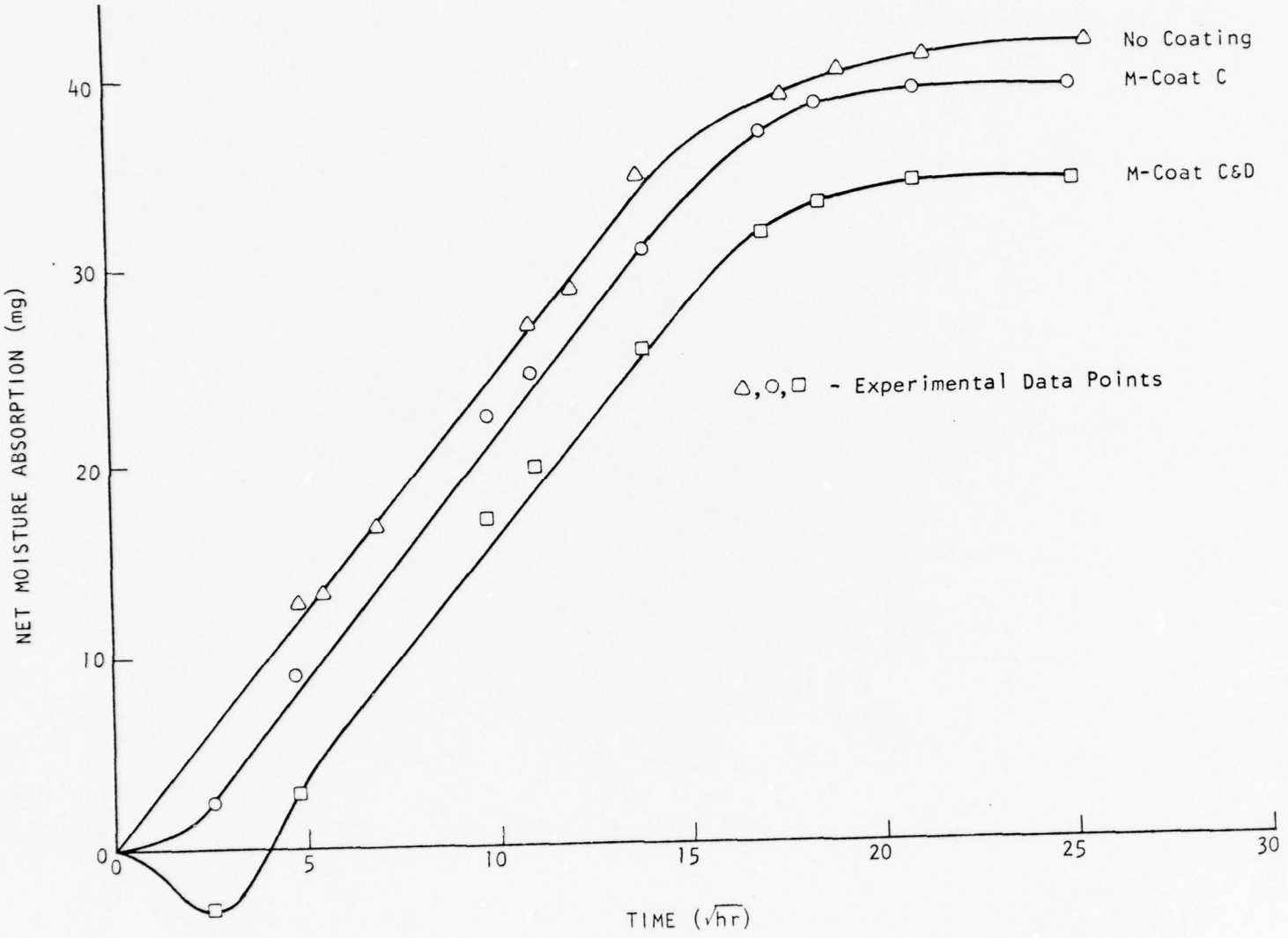

FIGURE 3. NET MOISTURE ABSORPTION OF ±45° GR/EP SPECIMEN UNDER 200°F AND 95% R.H.

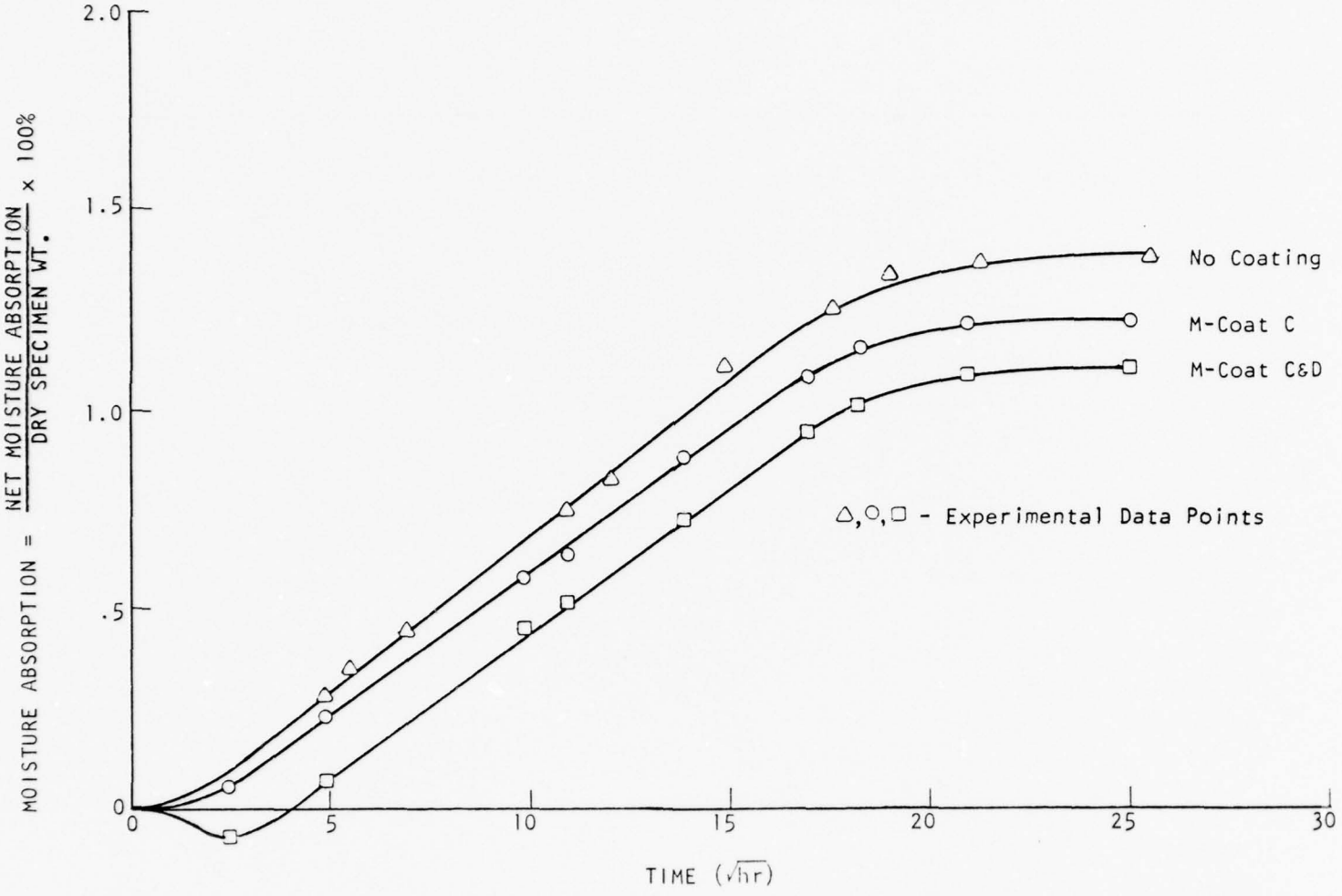

FIGURE 4. PERCENTAGE OF MOISTURE ABSORPTION OF 90° GR/EP SPECIMEN UNDER 200°F AND 95% R.H.

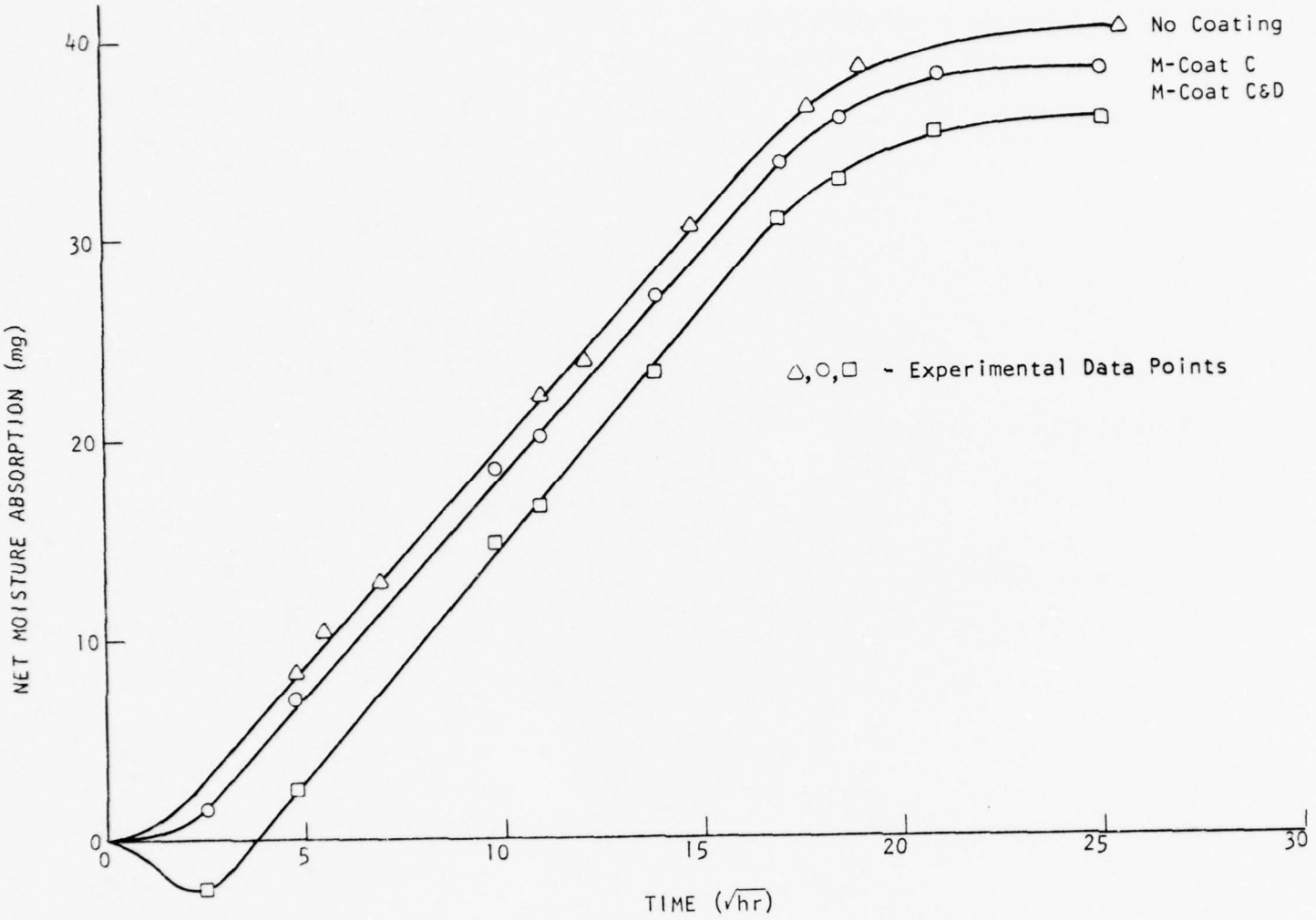

FIGURE 5. NET MOISTURE ABSORPTION OF 90° GR/EP SPECIMEN UNDER 200 F AND 95% R.H.

samples as compared with that of the uncoated samples, but the time to reach saturation seems unchanged. For each curve net moisture absorption is defined as wet minus dry specimen weight at time (t).

For the uncoated samples the diffusivity is around 6.2×10^{-6} in^2/hr for the 90° specimen and 6.8×10^{-6} in^2/hr for the ± 45° specimen. The edge effect of square samples was not considered. This compares to a diffusivity coefficient of 2.8×10^{-6} in^2/hr at 200°F and 90% R.H. for a T300/1034 ± 45° plate.[1]

All test specimens for this program had the same thickness, 0.10", as those of the moisture absorption samples. Thus, those specimens requiring moisture equilibrium at 200°F and 95% R.H. environment were conditioned to 95% saturation at the end of 22 days.

2.3 SPECIMEN CONDITIONING

Specimens were tested in the Shore-Western environmental test chamber which has six pin type loading fixtures. Quarter inch holes were drilled at the center of all specimen end tabs. A drilling position jig was designed to drill this quarter inch hole so that the center of the drilled hole and the center of the coupon was aligned within ± 0.005". Thus, a uniform stress field during testing was expected in the center gage section.

Before putting the specimen into the environmental conditioning chamber, scotch tape was wrapped around the specimen ends to protect the end tab bond area from moisture penetration. Some specimens had RTV rubber seal on top of the scotch tape. This preserved the bond strength, after conditioning, to enable creep-recovery and fatigue testing to proceed without premature end tab failures.

From Shen and Springer's[1] study and Vought's in-house work with adhesives in bonded joints, it is readily apparent that temperature acts as a catalyst in accelerating the moisture absorption rate without changing the maximum moisture content in the specimen at moisture equilibrium for a particular relative humidity. This information was used in the test program to shorten the specimen conditioning time. All specimens requiring moisture saturation were conditioned in a wet 200°F environment. This enabled the specimens to attain saturation in 22 days. This was below the specimen's "wet" glass transition temperature (Tg) of 231°F as determined by Differential Scanning Calorimeter Measurements.

All the specimens were conditioned to at least 95% saturation before they were tested. There are five humidity levels in this program: 50%, 57%, 71%, 79% and 95% relative humidity. These humidity conditions were attained by placing selected specimens in chambers containing saturated aqueous salt solutions.

A saturated aqueous solution in contact with some solid phase of the salt at a given temperature will maintain constant humidity in an enclosed space. The choice of compounds for attaining the previously mentioned relative humidity levels are given in the following table.

SOLID PHASE	SYMBOL	TEMPERATURE	% RELATIVE HUMIDITY
Ambient Condition		75°F	50%
Potassium Iodide	(KI)	200°F	57%
Potassium Bromide	(KBr)	200°F	71%
Potassium Chloride	(KCl)	200°F	79%
Sodium Fluoride	(NaF)	200°F	95%

3.0 MECHANICAL MEASUREMENT TECHNIQUES

3.1 STRAIN GAGE AND EXTENSOMETER

The ability of strain gages to measure strains in high temperature, high humidity environments is at present unproven. Moreover, it is desirable to use a biaxial strain gage on all ± 45° specimens to obtain shear compliance data. Therefore, a Micro-Measurement's strain gage, WK-00-250BG-350, which had shown extreme thermal stability in air to 167°F,[2] was bonded on six aluminum and three graphite/epoxy specimens. The specimens were placed in a 75°F/55% R.H. or a 200°F/95% R.H. environment. The gages were coated with M-coat C and/or D to ascertain if these materials can protect the gage in a hot, humid environment, thereby enabling their use in accurately recording the mechanical response of a composite in a severe environment during creep testing.

To insure the success of this program, a parallel effort was undertaken to develop an LVDT type of measurement device. Schaevitz's hermetically sealed LVDT's with CAS 025 signal conditioners were used. This system can withstand temperatures up to 250°F, and can measure up to 0.08" elongation. Its accuracy, as specified by the manufacturer is 0.000050". Two LVDT's and two holding plates were designed (Figure 6) as an extensometer measuring device. The gage length for the extensometer is two inches. The fixtures holding the LVDT's are made of chromic acid anodized aluminum to minimize corrosion of the fixture. The whole extensometer has a weight less than 440 grams and is weight balanced.

3.2 EVALUATION OF MEASUREMENT TECHNIQUES

The six aluminum and three ± 45° Gr/Ep specimens with the strain gages attached were conditioned for a two month period, during which environmental equilibrium of the Gr/Ep specimens was attained. Subsequent to this each type of specimen was put into the Shore-Western Environmental Test Chamber for creep-recovery testing at their respective environmental conditions. Figure 7 shows the test setup for those strain gaged and environmentally conditioned specimens. During testing, strain gage data was recorded by the Strain Gage Scanner on paper tape while extensometer voltage output signals were recorded on an X-Y plotter, a Digi-Strip recorder, and on the cassette in the HP 9815 calculator. Reduced data from the strain gage and extensometer measurements for a 200°F/95% R.H. conditioned specimen is plotted in Figure 8. They indicate that degradation

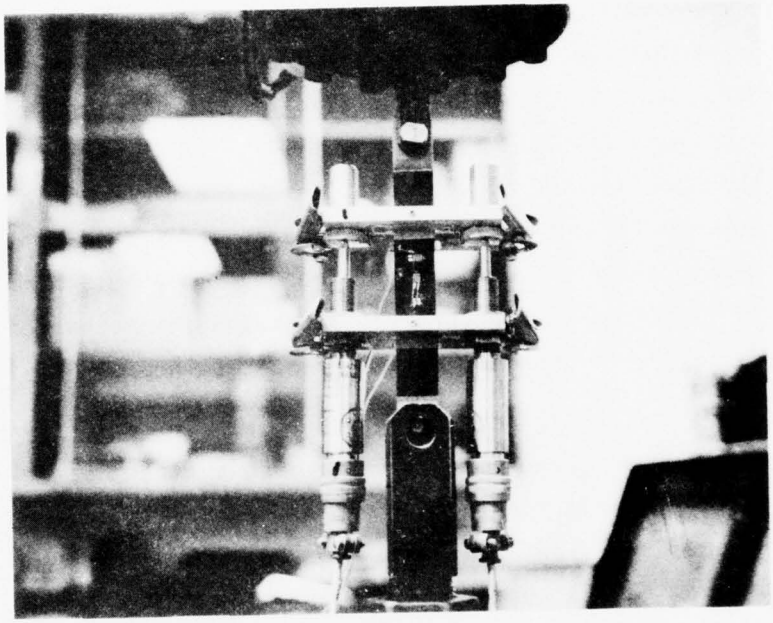

FIGURE 6. EXTENSOMETER SETUP ON GR/EP SPECIMEN.

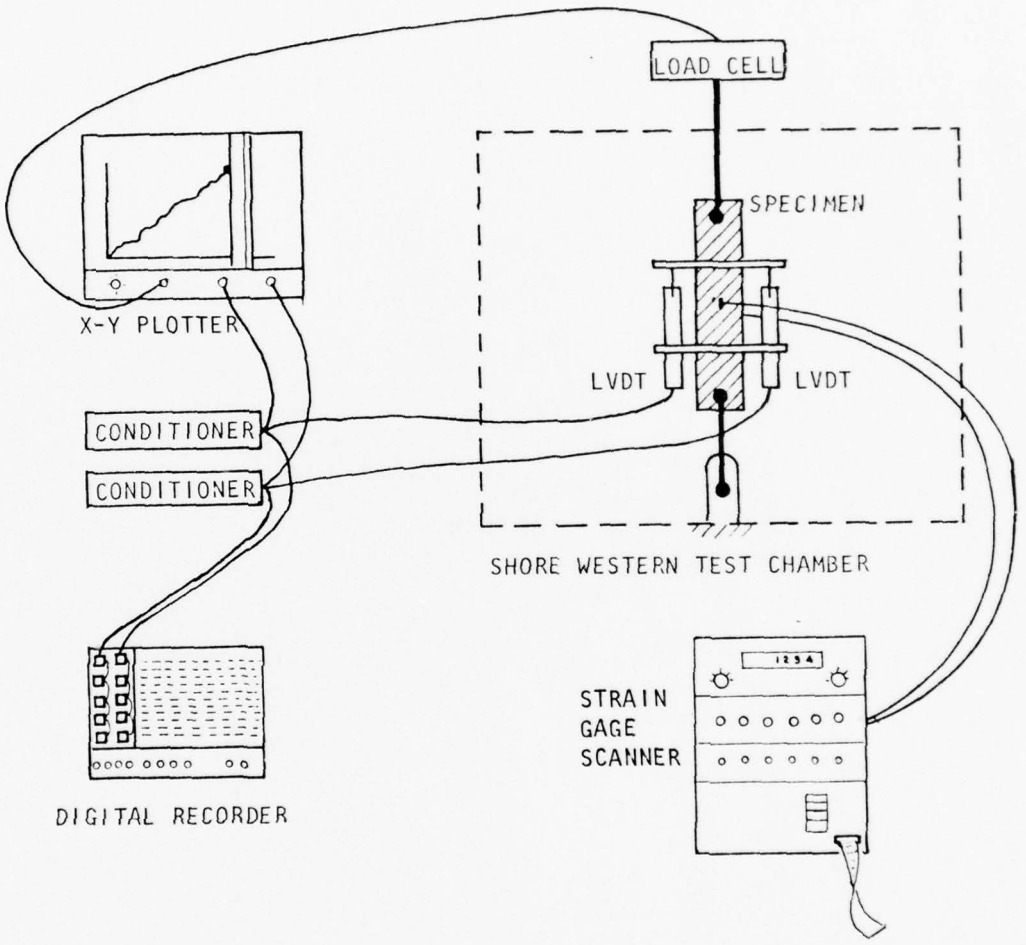

FIGURE 7. CALIBRATION OF MEASURING DEVICE FOR ENVIRONMENTAL TESTING.

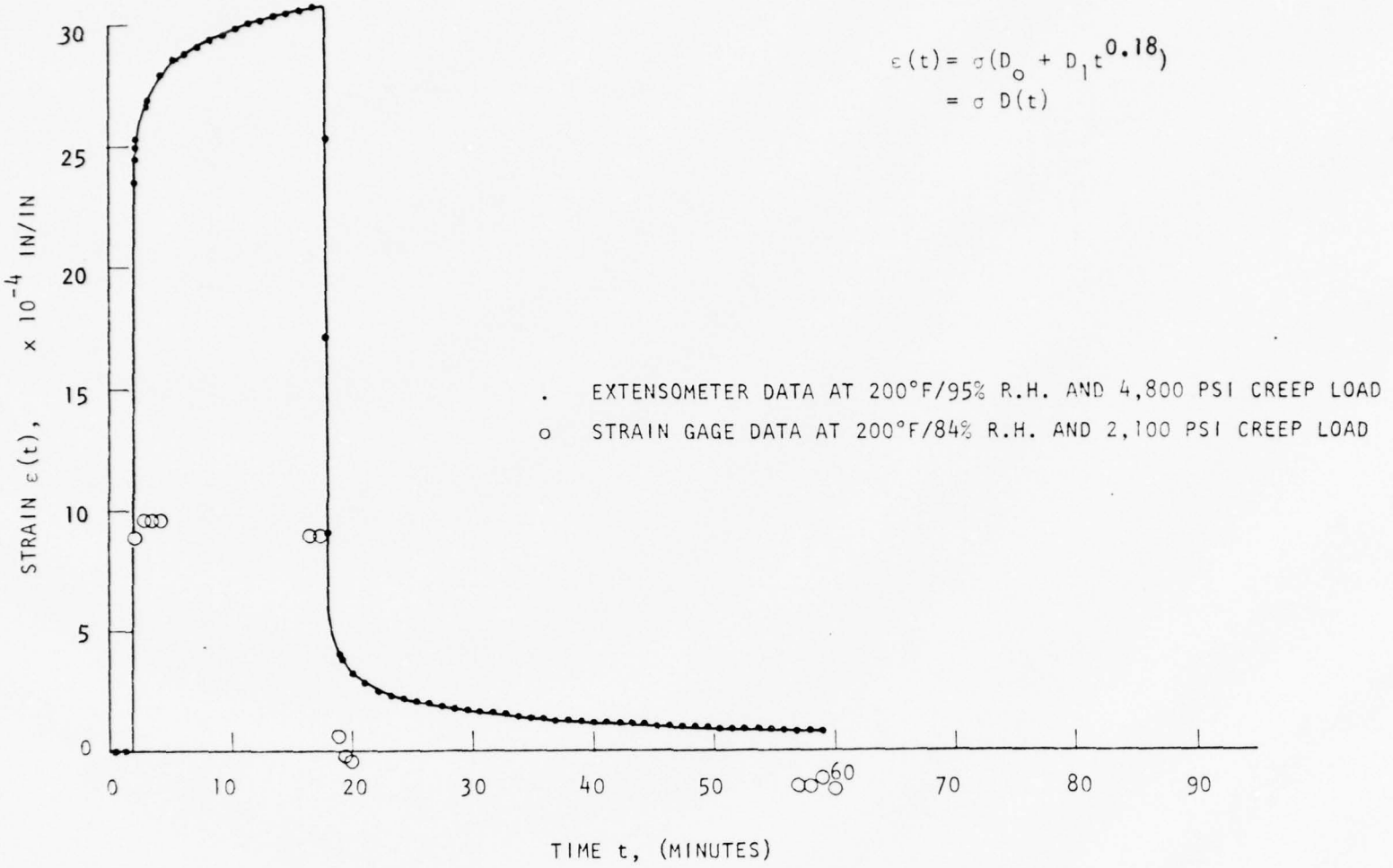

FIGURE 8. GR/EP COMPOSITE CREEP-RECOVERY TEST OF ±45° SPECIMEN CONDITIONED AT 200°F/95% R.H. ENVIRONMENT.

of the strain gage system by moisture at 200°F and 95% R.H. is obvious even though it is protected by M-coat C. The extensometer produces a more reliable creep-recovery curve in this severe environment and was used throughout this program to record all creep-recovery data. Since a one milli-volt output difference from the extensometer is equivalent to about ± 0.0000086", (a function of the environment), the extensometer has a calibrated recording accuracy up to ± 0.0000043 in/in strain.

4.0 REVIEW ON VISCOELASTIC COMPOSITE MATERIAL CHARACTERIZATION

4.1 ANALYSIS TECHNIQUE FOR CHARACTERIZING VISCOELASTIC COMPOSITE

The linear viscoelastic theory reviewed by Schapery[3] for composite materials is employed as the baseline analytical method to study the effect of time, temperature, and humidity on the mechanical behavior of AS/3501-6 material. In part, a quasi-elastic representation is employed to relate viscoelastic constitutive equations in an elastic format.

$$\begin{bmatrix} \varepsilon_1 \\ \varepsilon_2 \\ \gamma_{12} \end{bmatrix} = \begin{bmatrix} S_{11} & S_{12} & 0 \\ S_{12} & S_{22} & 0 \\ 0 & 0 & S_{66} \end{bmatrix} \begin{bmatrix} \sigma_1 \\ \sigma_2 \\ \tau_{12} \end{bmatrix} \tag{1}$$

Here, Cartesian coordinates 1-2 are used for the principal directions of the unidirtional lamina, (1-parallel to fiber; 2-perpendicular to fiber). Compliance, S_{ij}, may vary with time, temperature, and humidity and was determined in this program by testing of 0°, ±45°, and 90° specimens. The general form of S_{ij} often times can be represented in a power law form:

$$D(t, T, R.H.) = D_o + D_1 t^n \tag{2}$$

where t, T, and R.H. stand for time, temperature and relative humidity respectively. The time independent constants D_o, D_1, and n were evaluated based on our experimental results. Specifically, one can determine S_{11} and S_{22} from uniaxial creep-recovery tests of 0° and 90° specimens, respectively. They are related to the test data by

$$S_{11} = \frac{\varepsilon_1}{\sigma_1} \text{ and } S_{22} = \frac{\varepsilon_2}{\sigma_2} \tag{3}$$

where

σ_1 = Creep stress applied to 0° specimen
ε_1 = Creep strain experienced by 0° specimen
σ_2 = Creep stress applied to 90° specimen
ε_2 = Creep strain experienced by 90° specimen

Theoretically, shear compliance, S_{66}, can be determined[4] from the biaxial strain data obtained during the creep-recovery testing of a ± 45° specimen. As pointed out in Section 3.2 , strain gages were found to be unsatisfactory for measuring creep-recovery strain in severe environments. Thus, an alternate analytical procedure to obtain S_{66} is proposed and its validity is discussed in Section 4.2.

To evaluate S_{12}, we have the equation

$$S_{12} = -S_{11} \nu_{12} \tag{4}$$

Here, S_{11} is obtained from uniaxial creep-recovery test data of 0° specimens. The quantity ν_{12} can be obtained from biaxial measurements at specific temperatures (low R.H.) by using a strain gage technique. Variation of ν_{12} with humidity was assumed to be small. This assumption was based on the fact[5] that the Poisson's Ratio of epoxy resins is generally a weak function of time-temperature, and the humidity effect and temperature effect are roughly equivalent. Our test results, shown in Section 6.2, verify this assumption.

4.2 ANALYSIS OF SHEAR COMPLIANCE S_{66}

Because of the difficulty in obtaining accurate biaxial measurements of creep-recovery strains through strain gage techniques, an analytical technique was developed to evaluate the shear compliance S_{66} and its dependence on time, temperature and humidity from uniaxial test data from 0°, ± 45° and 90° specimens.

Hooke's law for homogeneous and orthotropic material in a plane stress state can be written as

$$\begin{bmatrix} \sigma_1 \\ \sigma_2 \\ \tau_{12} \end{bmatrix} = \begin{bmatrix} Q_{11} & Q_{12} & 0 \\ Q_{12} & Q_{22} & 0 \\ 0 & 0 & Q_{66} \end{bmatrix} \begin{bmatrix} \varepsilon_1 \\ \varepsilon_2 \\ \gamma_{12} \end{bmatrix} \tag{5}$$

which is the inverse form of the strain-stress relation given by equation (1) of Section 4.1. The components Q_{ij} (i.e., stiffness matrix) in equation (5) are related to Young's moduli, E_{11} and E_{22}, the shear modulus, G_{12}, and the major Poisson's ratio, ν_{12}, by

$$Q_{11} = E_{11}/\Delta$$

$$Q_{22} = E_{22}/\Delta$$

$$Q_{12} = \nu_{12}\, E_{22}/\Delta$$

$$Q_{66} = G_{12} \tag{6}$$

where

$$\Delta = 1 - \nu_{12}^2 \frac{E_{22}}{E_{11}}$$

From laminated plate theory for a composite, the stiffness matrix, Q'_{ij}, for a mid-plane symmetric ±45° laminate in X-Y coordinates is

$$\begin{bmatrix} \sigma_x \\ \sigma_y \\ \tau_{xy} \end{bmatrix} = \begin{bmatrix} Q'_{11} & Q'_{12} & 0 \\ Q'_{12} & Q'_{22} & 0 \\ 0 & 0 & Q'_{66} \end{bmatrix} \begin{bmatrix} \varepsilon_x \\ \varepsilon_y \\ \gamma_{xy} \end{bmatrix} \tag{7}$$

with

$$\begin{aligned} Q'_{11} &= Q'_{22} = 1/4\ (Q_{11} + Q_{22} + 2Q_{12} + 4Q_{66}) \\ Q'_{12} &= 1/4\ (Q_{11} + Q_{22} + 2Q_{12} - 4Q_{66}) \\ Q'_{66} &= 1/4\ (Q_{11} + Q_{22} - 2Q_{12}) \end{aligned} \tag{8}$$

Under uniaxial load $(\sigma_x, 0, 0)^T$ the ±45° specimen will have the uniaxial compliance

$$\frac{1}{E_{xx}} = \frac{\varepsilon_x}{\sigma_x} = \frac{Q'_{11}}{Q'^2_{11} - Q'^2_{12}} \tag{9}$$

By introducing equations (6) and (8) into equation (9) and rearranging the terms, one obtains the shear compliance as a function of E_{11}, E_{22}, ν_{12} and E_{xx}. Thus,

$$S_{66} = \frac{1}{G_{12}} = 4\left[\frac{1}{E_{xx}} - \frac{1 - (E_{22}/E_{11})\nu_{12}^2}{E_{11} + E_{22}(1 + 2\,\nu_{12})}\right] \tag{10}$$

Quantities E_{11}, E_{22}, and E_{xx} are measurable from 0°, 90°, and ±45° tests respectively. Thus, the shear compliance S_{66} can be evaluated if ν_{12} is known.

Unfortunately, ν_{12} is not a directly measurable quantity because of the limitation of biaxial strain gage test techniques in severe moisture, temperature environments. However, we can assume a ν_{12} value based on the following two observations. First, the shear compliance is not sensitive to variations of ν_{12} value. For example, given a typical Gr/Ep composite with $E_{11} = 20 \times 10^6$ psi, $E_{22} = 1.2 \times 10^6$ psi, and $E_{xx} = 2.4 \times 10^6$ psi, the sensitivity of S_{66} as a function of ν_{12} can be determined by use of equation (10). The results are presented in Table 2. Inspection of Table 2 reveals the insensitivity of S_{66} to sizable changes in ν_{12} value. A 36% variation in the value of ν_{12} results in only a .18% error in S_{66}. Second, a representative value of ν_{12} with respect to temperature can be obtained by testing a 0° specimen without regard to humidity. A minor effect of humidity on ν_{12} is anticipated based on the work of Schapery[5] where he showed that epoxy's creep or relaxation Poisson's ratio vary between .36 and .39 over a twelve decades of time scale (minutes). It is also interesting to note that the output strain of a ± 45° test is above 8×10^{-4} in/in while the extensometer strain sensitivity is $\pm 4.3 \times 10^{-6}$ in/in. Thus, the inherent experimental error is

$$\text{Experimental Error} = \frac{4.3 \times 10^{-6}}{8 \times 10^{-4}} = .5\%$$

This .5% experimental error can easily override the .18% error in S_{66} due to an incorrect ν_{12} value.

TABLE 2. SENSITIVITY STUDY OF SHEAR COMPLIANCE S_{66}.

POISSON RATIO ν_{12}	.28	.34	.38
SHEAR COMPLIANCE S_{66} $(10^{-6}\ PSI^{-1})$	1.48465	1.48624	1.48734
RATIO $\frac{S_{66}}{S_{66} \text{ at } \nu_{12} = .28}$	1.00000	1.00107	1.00181

5.0 MECHANICAL CHARACTERIZATION TEST

5.1 TEST EQUIPMENT AND DATA ACQUISITION SYSTEM

All the mechanical tests of this program were conducted in the Structures and Materials Laboratory of Vought's Advanced Technology Center. The purpose of each piece of equipment used in the creep-recovery and fatigue tests is briefly summarized as follows:

- Shore-Western Environmental Test Machine - This machine can create temperatures in the range of -100°F to 450°F and humidity in the range of 0% to 98% R.H. simultaneously (up to 210°F). It has a 5000 lb. static load capacity and 0-30 Hz dynamic load frequency. Six load stands are in the machine. Three of these are dead weight load stands while the remaining three are hydraulic load stands. They can be operated simultaneously.
- Digi-Strip Recorder - This recorder has thirteen recordable channels with scan intervals of 1, 2, 4, 10, 20, and 40 minutes. It is connected to the HP 9815 calculator.
- HP 9815 Calculator - This is a programmable calculator equipped with a 2008 program step capability. It has built-in tape drive and allows permanent recordings of programs and data. Its tape cartridge will record data that are sent to the calculator from the Digi-Strip recorder during the static or creep-recovery test. Later on, data stored in the cassette can be processed to produce test curves through the HP 9862A X-Y plotter.
- Extensometer - As discussed in Section 3, this measuring device has two LVDT's, Model GCA-121-050, and two signal conditioners, CAS 025, which will measure the displacement over a two inch gage length of the specimen. The voltage signal is sent to either the Digi-Strip or X-Y plotter or both.

The recordable voltage accuracy for the Digi-Strip is in milli-volts as is the data accuracy of the cassette. A one milli-volt output difference from the extensometer is equivalent to about ± 0.0000086" (a function of the environment) or ±0.0000043 in/in strain fluctuation over a two inch gage length area. The overall creep-recovery test and data acquisition system is shown in Figure 9.

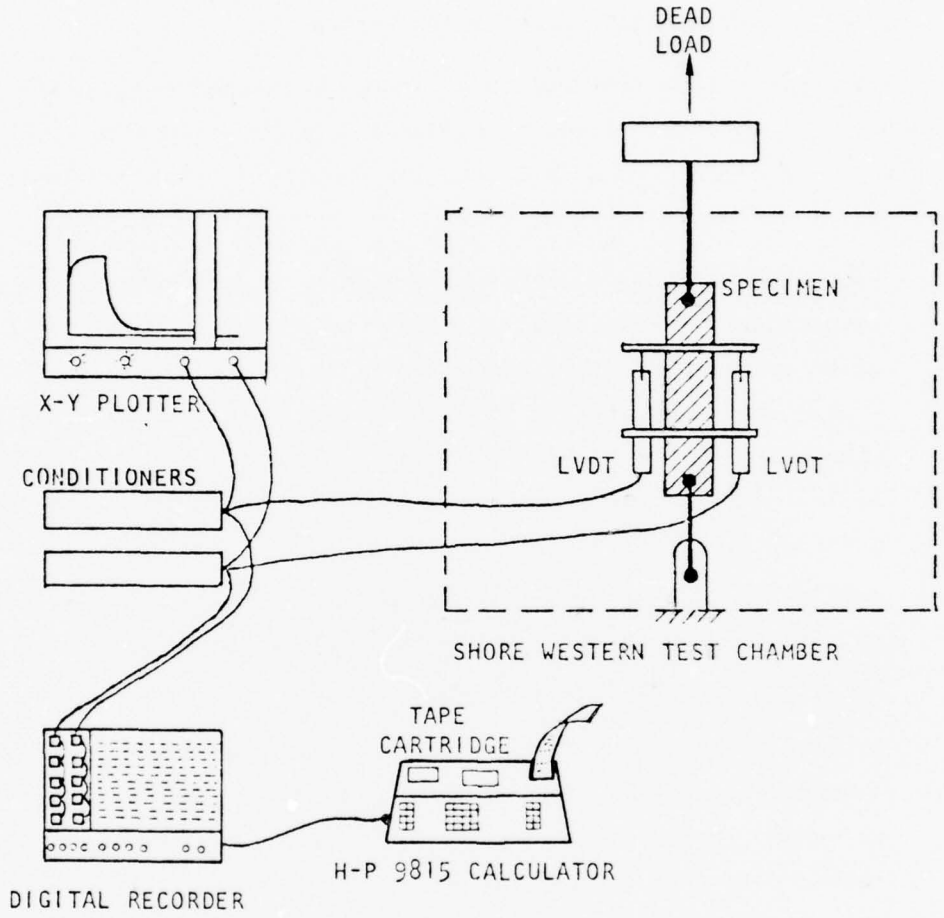

FIGURE 9. CREEP-RECOVERY TEST AND DATA ACQUISITION SYSTEM.

5.2 SELECTION OF TEST ENVIRONMENT

Since the glass transition temperature (T_g) of the AS/3501-6 system decreases from 375°F to approximately 230°F once the laminate has attained moisture equilibrium in a 95-100% relative humidity environment, we have defined our extreme environments for the test program as 200°F at 95% R.H. and 75°F at room ambient.

The compliance coefficients S_{ij} (t, T, R.H.) depend on both temperature and humidity. Several combinations of temperature and humidity are necessary for the determination of S_{ij}. These have been defined for test purposes as:

(T°F, % R.H.) = (200, 95), (200, 79), (200, 71)
(200, 57), (200, 50)
(188, 95), (188, 79), (188, 71)
(188, 57), (188, 50)
(176, 95), (176, 79), (176, 71)
(176, 57), (176, 50)
(158, 95), (158, 79), (158, 71)
(158, 57), (158, 50)
(132, 95), (132, 79), (132, 71)
(132, 57), (132, 50)
(75, 95), (75, 79), (75, 71)
(75, 57), (75, 50)

The temperature selection above is based on Figure 10 where the Arrhenius activation energy equation and power law equation for creep strain are used to derive the temperature and creep strain relation and the temperatures are selected with equal creep strain between them.

5.3 STATIC STRENGTH TEST

Static strength tests in various environments for 0°, ±45° and 90° specimens have been conducted. These tests were to provide the baseline data for creep-recovery and fatigue tests. The results are shown in Table 3. The comparative data of Gr/Ep AS/3501-5 from Browning[6] are also listed in the table although the test environment and test technique are different. For high strength (0°) specimens, and ± 45° specimens, tests were conducted on a MTS machine with a 100,000 lb. load cell. Hydraulic grip pressure was adjusted to around 600 psi during the testing. Wet towels and a heating pad were wrapped around the specimen to produce the desired test environment and to prevent the environmentally conditioned specimens from desorbing during the test. Temperature was monitored by thermo-

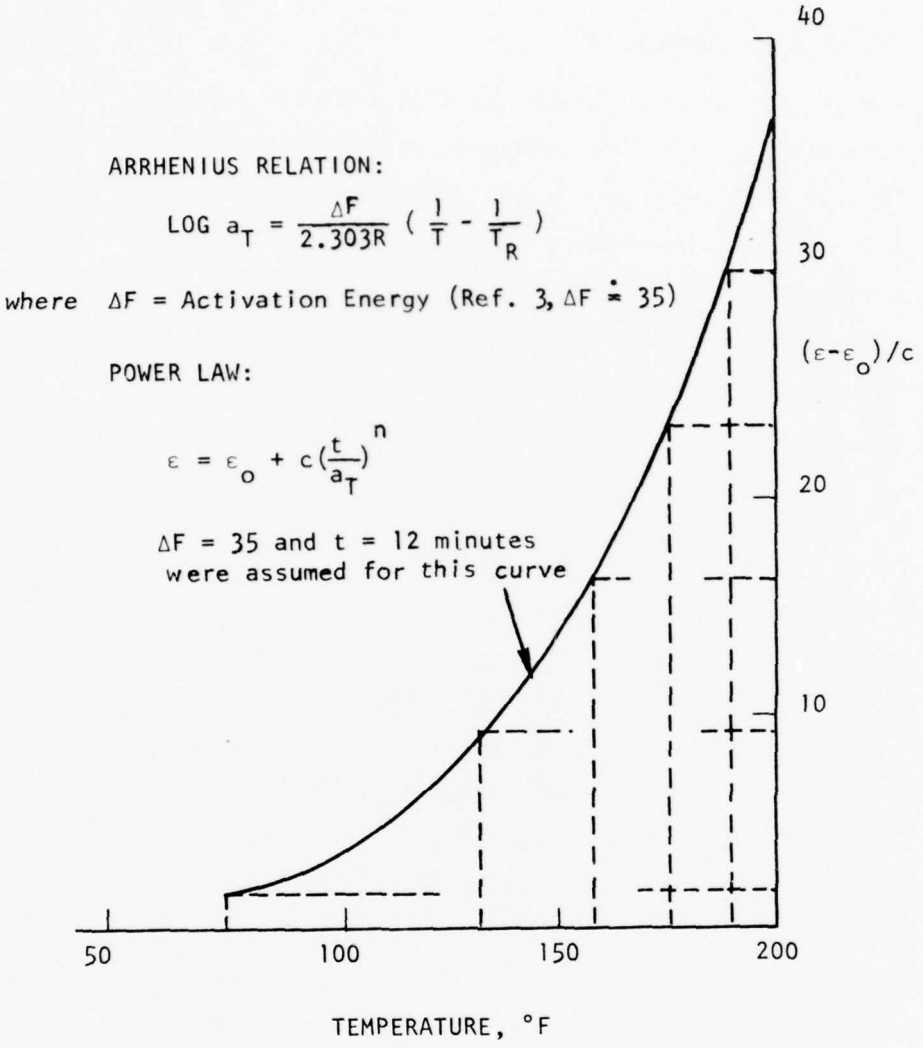

FIGURE 10. DETERMINATION OF TEMPERATURE LEVELS FOR THE TEST PROGRAM.

TABLE 3. STATIC STRENGTH OF GR/EP AS/3501-6 (V_f = 66%).

SPECIMEN		TEST ENVIRONMENT		CONDITIONED ENVIRONMENT		ULTIMATE STRENGTH (ksi)	ULTIMATE STRAIN (% IN/IN)	FAILURE MODE OR LOCATION
ORIEN-TATION	ID	TEMP. (°F)	HUMIDITY (% R.H.)	TEMP. (°F)	HUMIDITY (% R.H.)			
0°	14	75	55	75	55	226	---	Fiber Split
	1	75	55	75	55	211	---	
	12	132	95	200	95	223	---	Fiber Split
	5	132	95	200	95	243	---	
	10	200	95	200	95	214	---	Fiber Split
	3	200	95	200	95	229	---	
±45°	12	75	55	75	55	27.7	---	Gage section failed
	13	75	55	75	55	27.8	---	
	16	132	95	200	95	26.1	---	Gage section failed
	17	132	95	200	95	24.5	---	
	14	200	95	200	95	18.2	---	Gage section failed
	15	200	95	200	95	23.0	---	
90°	1	75	Dry	75	Dry	6.96	---	Tab end section failed
	2	75	Dry	75	Dry	6.41	---	Tab end section failed
	12	132	95	200	95	2.67	.275	Tab end section failed
	17	132	95	200	95	3.30	.311	Gage section failed
	19	200	95	200	95	3.02	.289	Gage section failed
	20	200	95	200	95	3.09	.298	Tab bondline failed
*COMPARATIVE DATA OF GR/EP AS/3501-5 (Reference 6)								
0°		RT	---	160	95	194	1.13	
		200	Dry	160	95	213	---	
±45°		RT	---	160	75	30.8	---	
		250	Dry	160	75	19.0	---	
90°		RT	---	160	95	2.9	.23	
		200	Dry	160	95	2.2	.32	

*V_f = 63 %

couples that were attached to the center of the specimen. Ninety degree specimens were tested in the Shore-Western machine which is capable of producing the desired environment in the test chamber.

Results in Table 3 indicate that data scatter is a function of failure location and failure mode. For 0° specimens, the failure process is fiber splitting. All ± 45° specimens failed in the center portion of the specimen and their failure process was repeatable. Thus, the data scatter is smaller. For 90° specimens, some failed near the end of the end tab while others failed at the center gage section. Overall, results are similar to those experienced by other researchers for Gr/Ep material.

5.4 CREEP-RECOVERY TEST

Creep-recovery testing of AS/3501-6 composite material was performed in the Shore-Western environmental test machine. Hot wet air was circulated and distributed inside the test chamber by a 1/3 horse power fan. There are sensors to control temperature and humidity and about fifteen minutes are required for the test chamber to attain equilibrium at the desired environment. Preliminary tests at 200°F/95% R. H. environment indicated that the test assembly including specimen, extensometer and fixture linkages required at least thirty minutes to adjust to the new temperature level and to become stabilized in this environment. This thirty minute period is called the thermal conditioning period. After the test system was stabilized, the specimen was loaded and unloaded several times (3 to 15 times at creep stress level) at the rate of 2 cycles per minute. This exercise is called mechanical conditioning and is important, in that it not only mechanically conditions the specimen in the chamber, but also enables one to verify the stability of the fixture linkage systems so that it will yield reproducible test results. Figure 11 shows the typical thermal conditioning and the mechanical conditioning of a 90° specimen in a 200°F/95% R.H. environment. The specimen assembly is considered thermally stabilized in that environment when the two LVDT traces become horizontal during thermal conditioning. Three-cycle mechanical conditioning is also shown in Figure 11 which is to assess the effect of internal microcracking in the specimen and to develop it to a fixed level before creep and recovery testing. We consider the microcracking stabilized when the peaks of the neighboring cycles are of the same height.

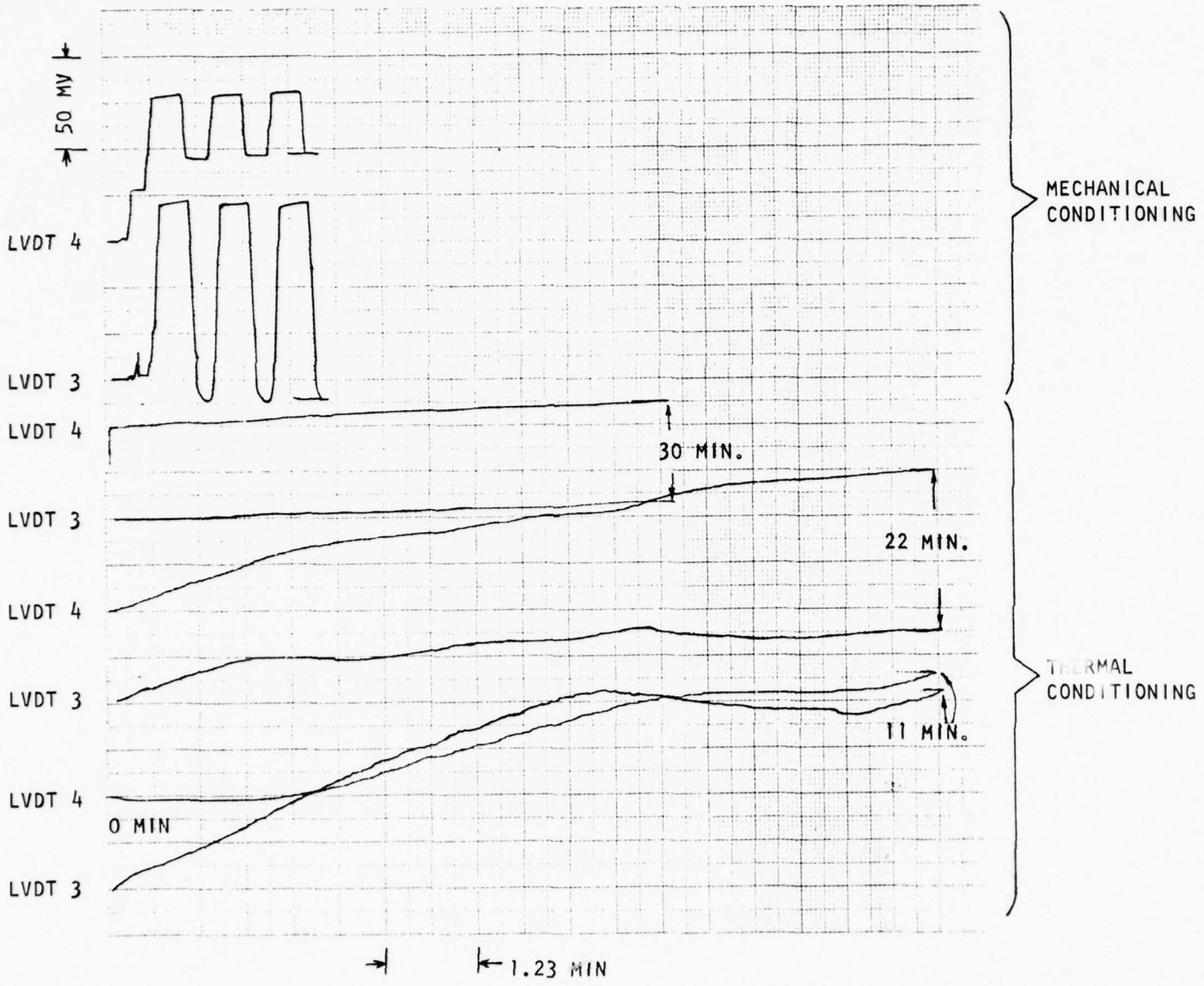

FIGURE 11. STABILITY TEST OF THERMAL CONDITIONING AND MECHANICAL CONDITIONING FOR TEST SYSTEM.

The gage length of the extensometer is two inches as noted previously. An assembly jig has been made and is employed to clamp the extensometer onto the specimen (Figure 12), assuring the two inch gage length is maintained over the appropriate length of the specimen. The extensometer clamping spring force will exert about 1000 psi pressure normal to the specimen's surface at the contact points.

After the specimen and extensometer assembly have attained thermal and mechanical equilibrium, a three cycle creep-recovery test is conducted. The test data were recorded using the Digi-Strip recorder. Creep-recovery repeatability is consistently observed between the second and third load-unload cycles. An adequate creep-recovery cycle has been determined to be one hour (fifteen minutes of creep and forty-five minutes of recovery). This load-unload time arrangement has been found to be most economical for the evaluation of creep-recovery data as far as a power law is concerned. Figure 13 depicts such a creep-recovery test arrangement.

Creep-recovery tests were conducted on $\pm 45°$ and $90°$ specimens. Typical results are shown in Figures 14 through 18. Two stress levels, 10% and 20% of ultimate stress, were used for testing $\pm 45°$ specimens in order to ascertain the linearity of the material. Stress levels of 25% and 50% of ultimate were used for $90°$ specimen testing.

Inspection of the data revealed that the test results from $\pm 45°$ specimens are somewhat more consistent than that of the $90°$ specimen. This difference in the test quality is caused by two factors. The first is that the instantaneous modulus of a $\pm 45°$ specimen is about 3×10^6 psi while that of a $90°$ specimen is about 1.6×10^6 psi. Thus, any slight disturbance such as flow vibration or fan blowing in the test chamber during the test will be more likely to be observed in the deflection response of the $90°$ specimen vs. that for the $\pm 45°$ specimen. The second factor is that the dead weight creep load on a $90°$ specimen is in the 50 to 100 lb. range while that of a $\pm 45°$ specimen is in the 200 to 400 lb. range. Hence, the test assembly is more susceptible to mechanical disturbances when testing $90°$ specimens.

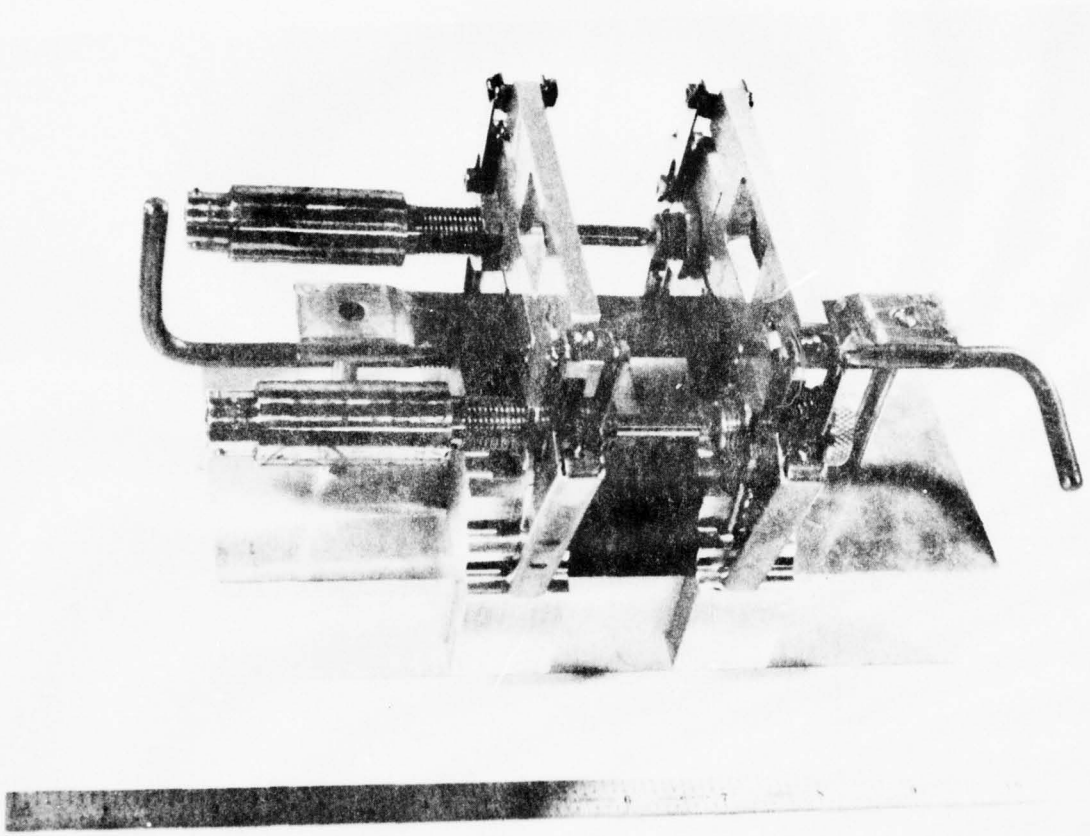

FIGURE 12. EXTENSOMETER AND SPECIMEN ASSEMBLY JIG.

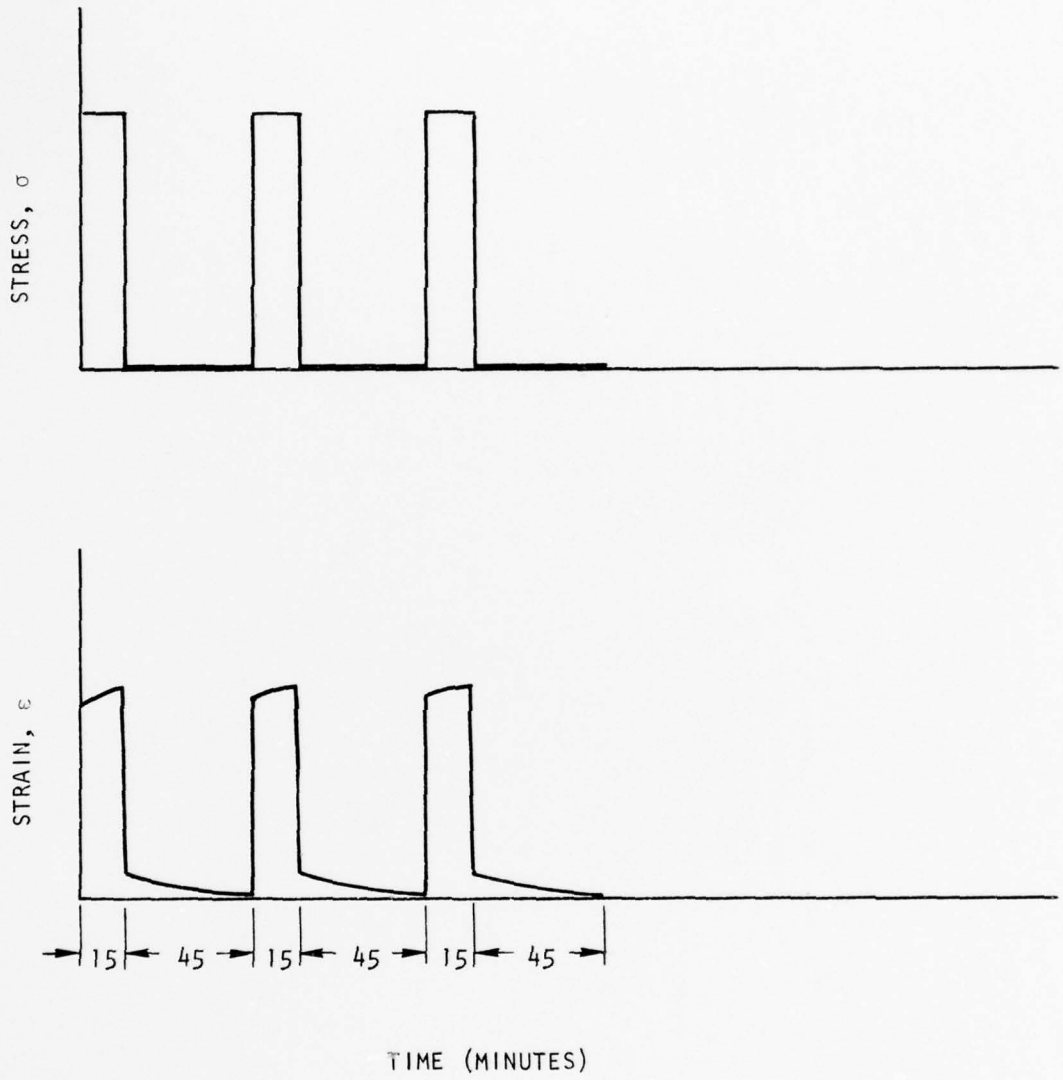

FIGURE 13. CREEP-RECOVERY TEST OF VISCOELASTIC MATERIAL.

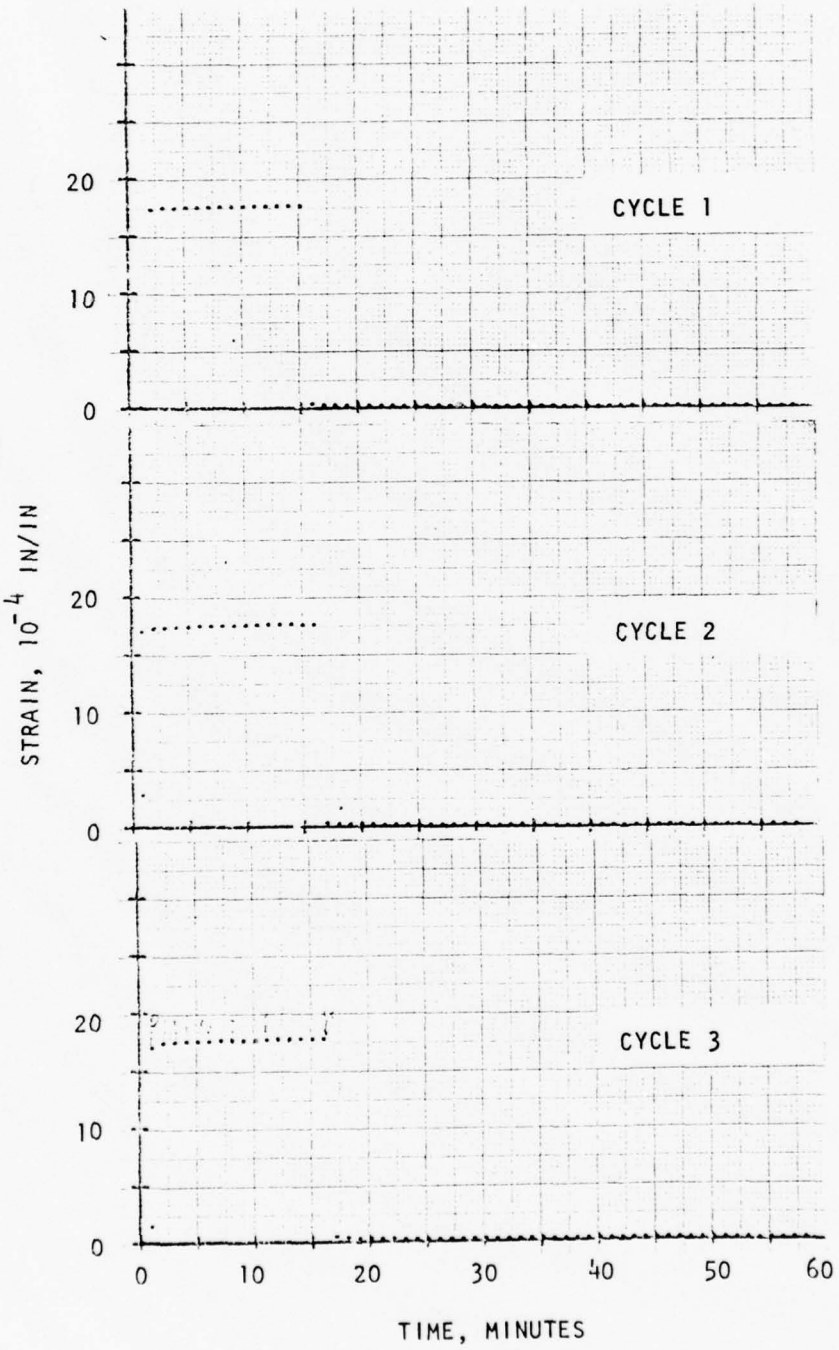

FIGURE 14. CREEP-RECOVERY TEST OF ±45° SPECIMENS AT STRESS LEVEL OF 4.94 KSI AND 75°F/50% R.H. ENVIRONMENT.

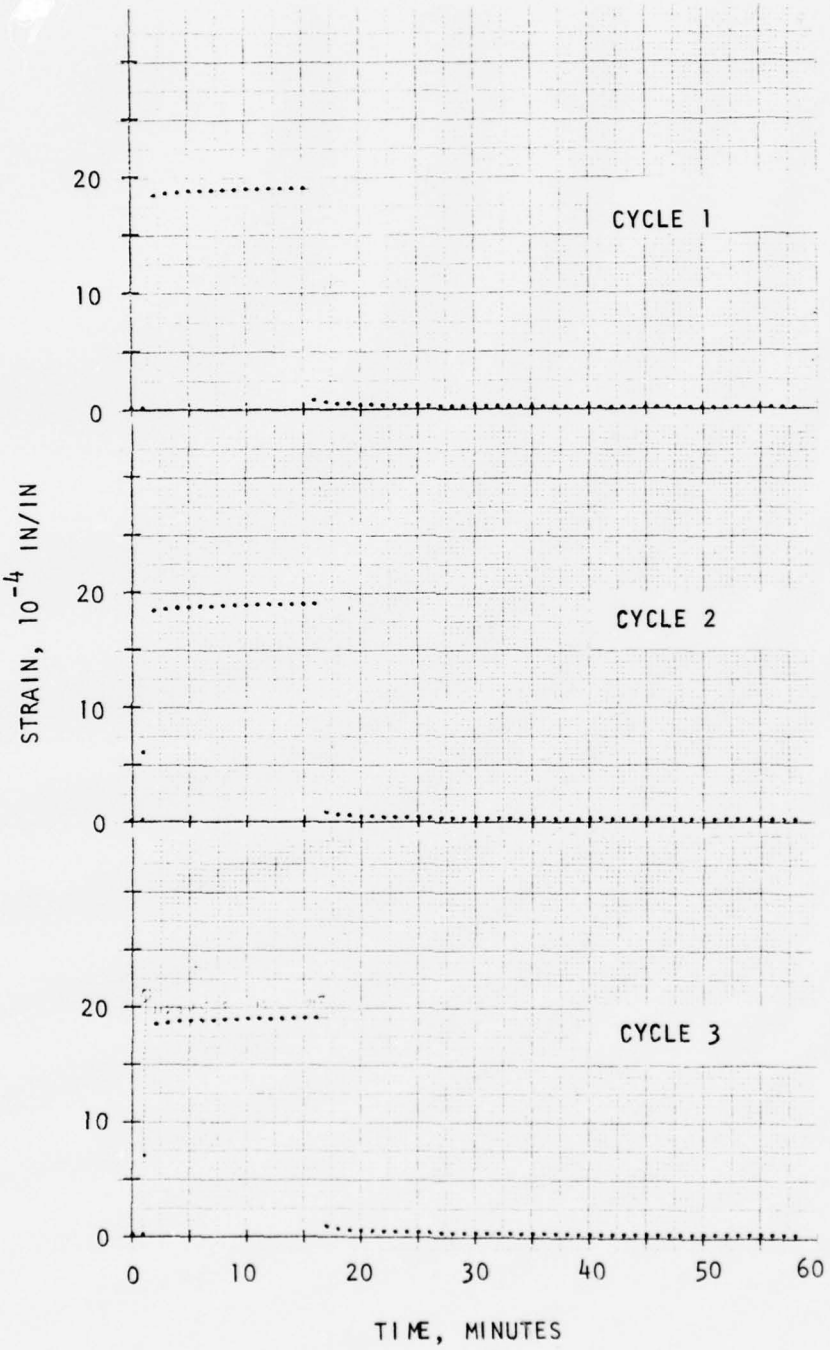

FIGURE 15. CREEP-RECOVERY TEST OF ±45° SPECIMENS AT STRESS LEVEL OF 5.17 KSI AND 75°F/50% R.H. ENVIRONMENT.

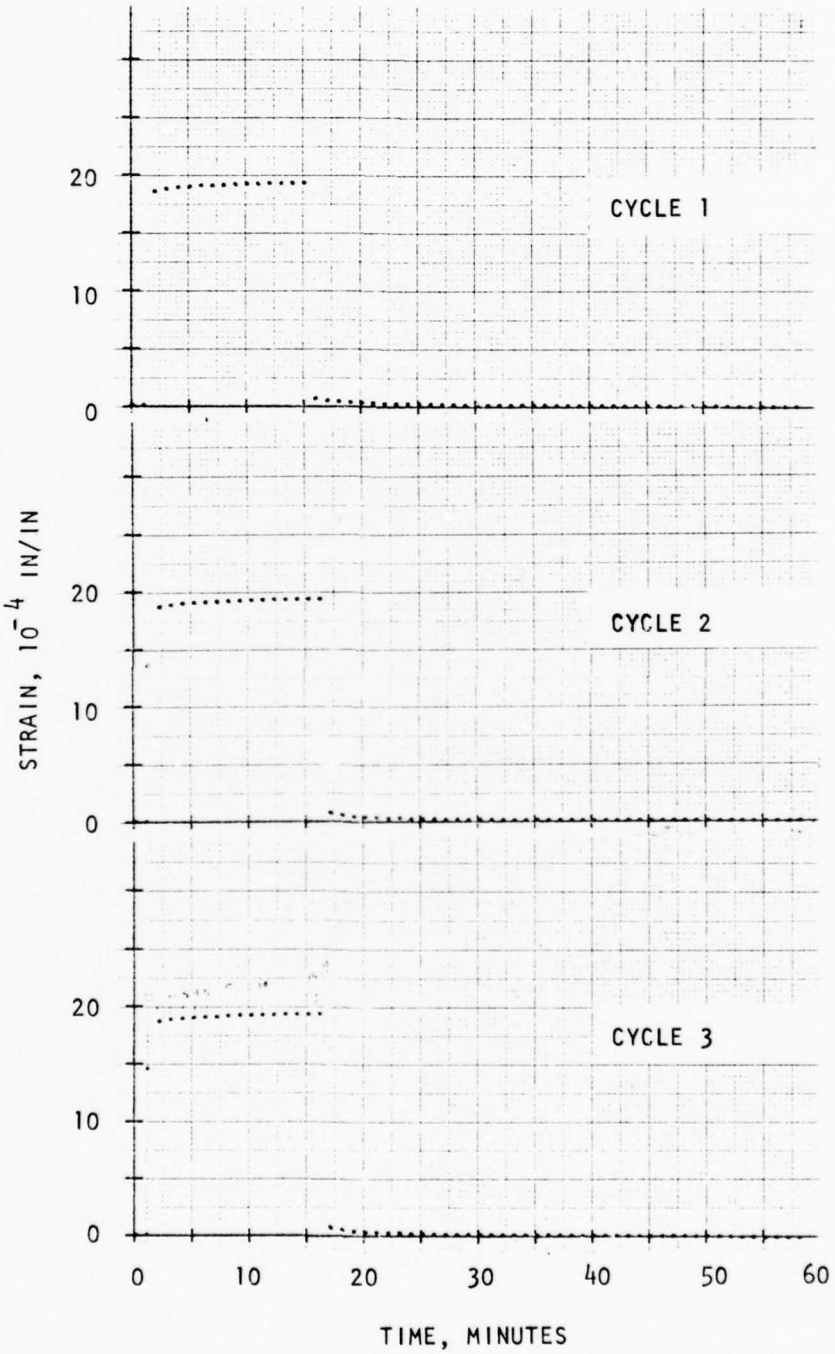

FIGURE 16. CREEP-RECOVERY TEST OF ±45° SPECIMENS AT STRESS LEVEL OF 4.98 KSI AND AND 75°F/71% R.H. ENVIRONMENT.

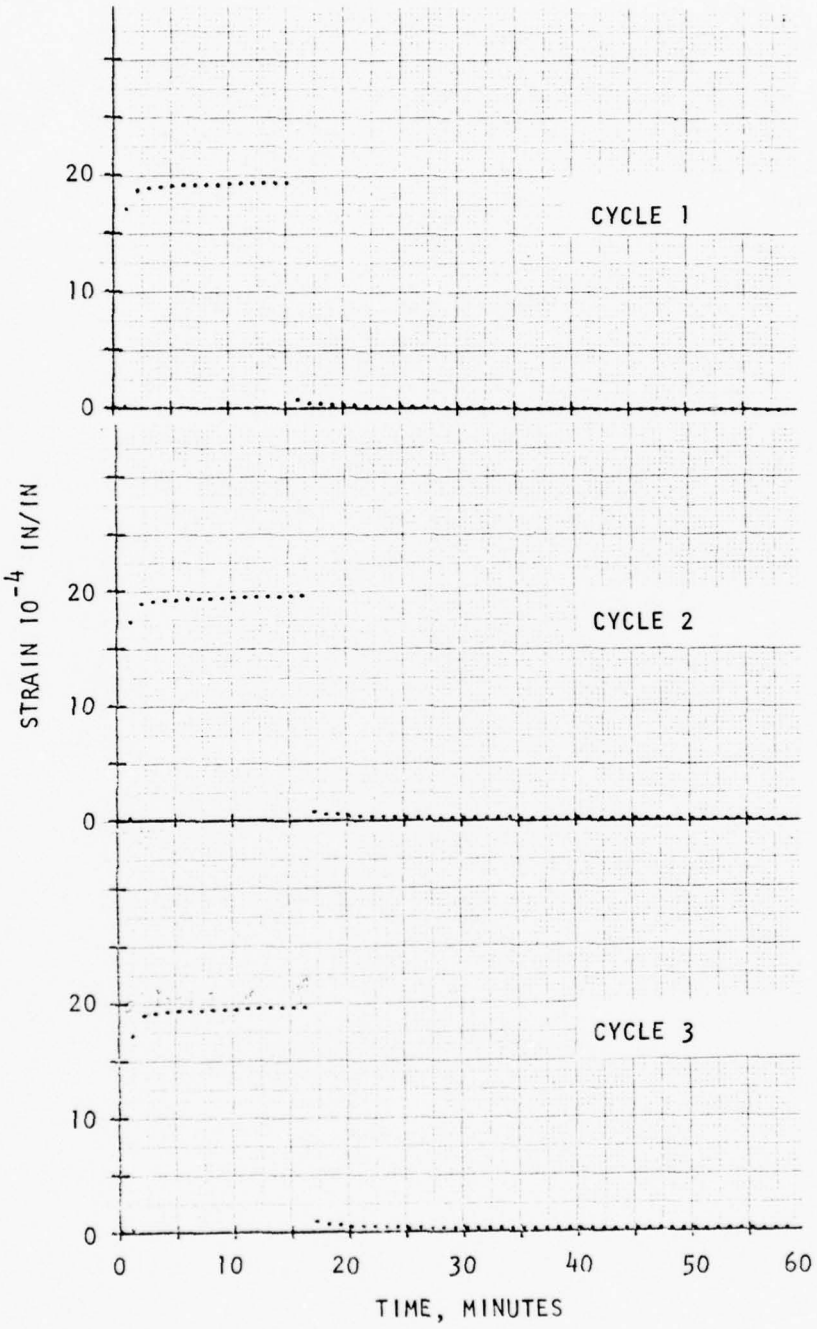

FIGURE 17. CREEP-RECOVERY TEST OF ±45° SPECIMENS AT STRESS LEVEL OF 4.90 KSI AND 75°F/79% R.H. ENVIRONMENT.

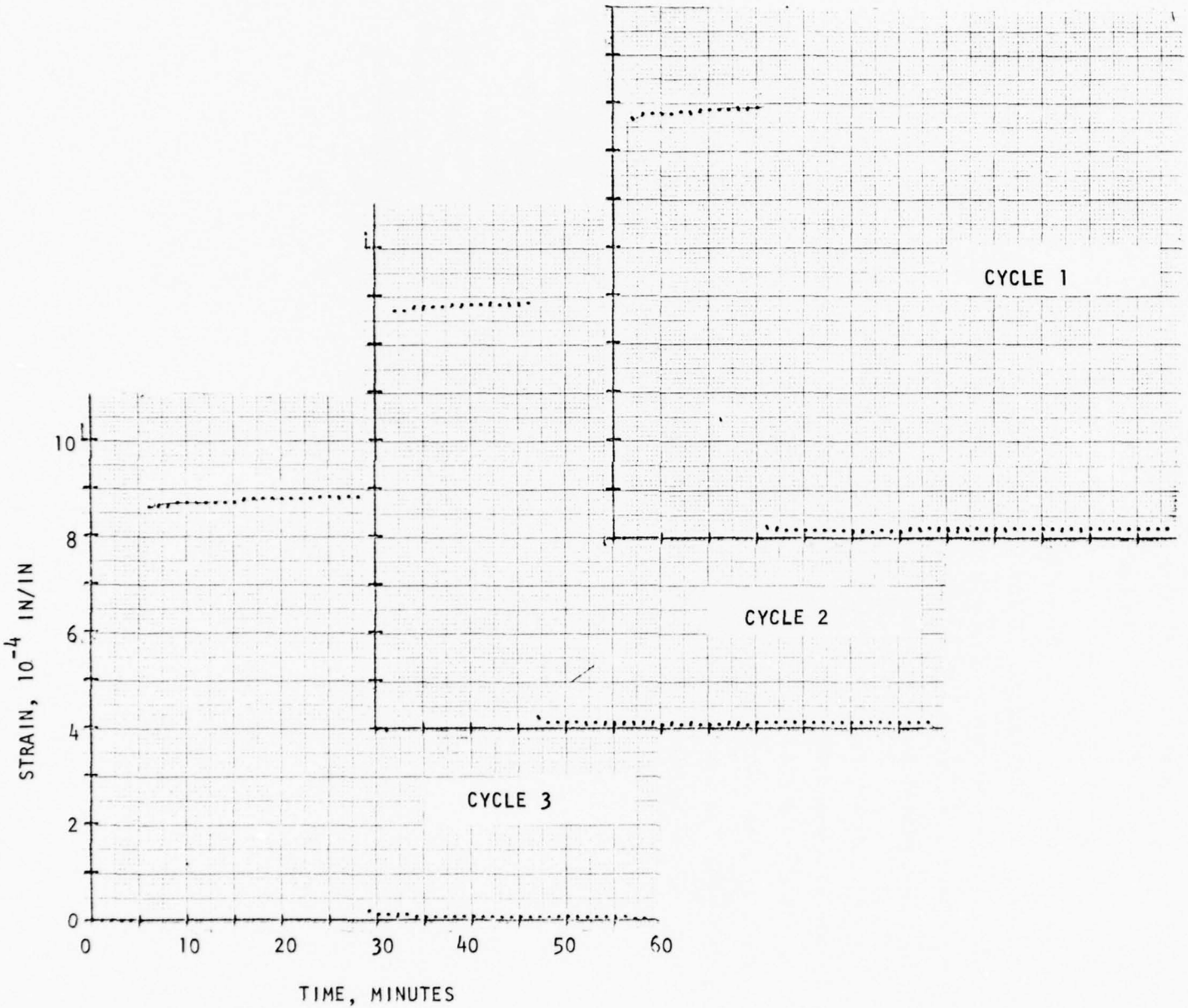

FIGURE 18. CREEP-RECOVERY TEST OF 90° SPECIMEN AT STRESS LEVEL OF 1.37 KSI AND 80°F/50% R.H ENVIRONMENT.

5.5 FATIGUE TEST

The fatigue test technique in a severe environment has been established and evaluated. The longitudinal deformation in the specimen was monitored by the extensometers shown in Figure 6 in a manner identical to that for the creep-recovery tests. The cyclic frequency of all fatigue testing has been set at 3 hertz. The displacement over the two inch gage length of the specimen is recorded continuously on a HP 7402A strip chart recorder. Thermocouples seem to create some disturbance on the LVDT reading since they were crossing each other in the specimen's gage section. Hence, we decided to have four specimens monitored by extensometer and another four specimens by thermocouples for each test environment and each stress level.

Preliminary fatigue test results show that the extensometer is a stable, repeatable measuring system at 3 Hz. Figure 19 is a sample of selected output from the strip chart recorder for various times during the test. The horizontal scale is time. The vertical scale represents deformation and is set at 20 mv per division. The two horizontal ink strips represent the two LVDT headings which were located on each side of the specimen during the test. The gradual increase in mean strain and strain amplitude is also shown in Figure 19. The mean strain increases according to the power law given by equation (2). The two LVDT extensometer systems have the advantages of monitoring the eccentricity of the loading pins centerline with respect to the specimen's centerline. Figure 20 shows that after loading, points A & B at the side of the specimen moved to points A' and B' respectively. From the test data shown in Figure 19, we see that $\overline{AA'}$ and $\overline{BB'}$ can be calculated to be 2131 μin and 2199 μin respectively prior to the specimen's failure. This enables one to ascertain the importance of eccentric loading effects in all subsequent fatigue testing.

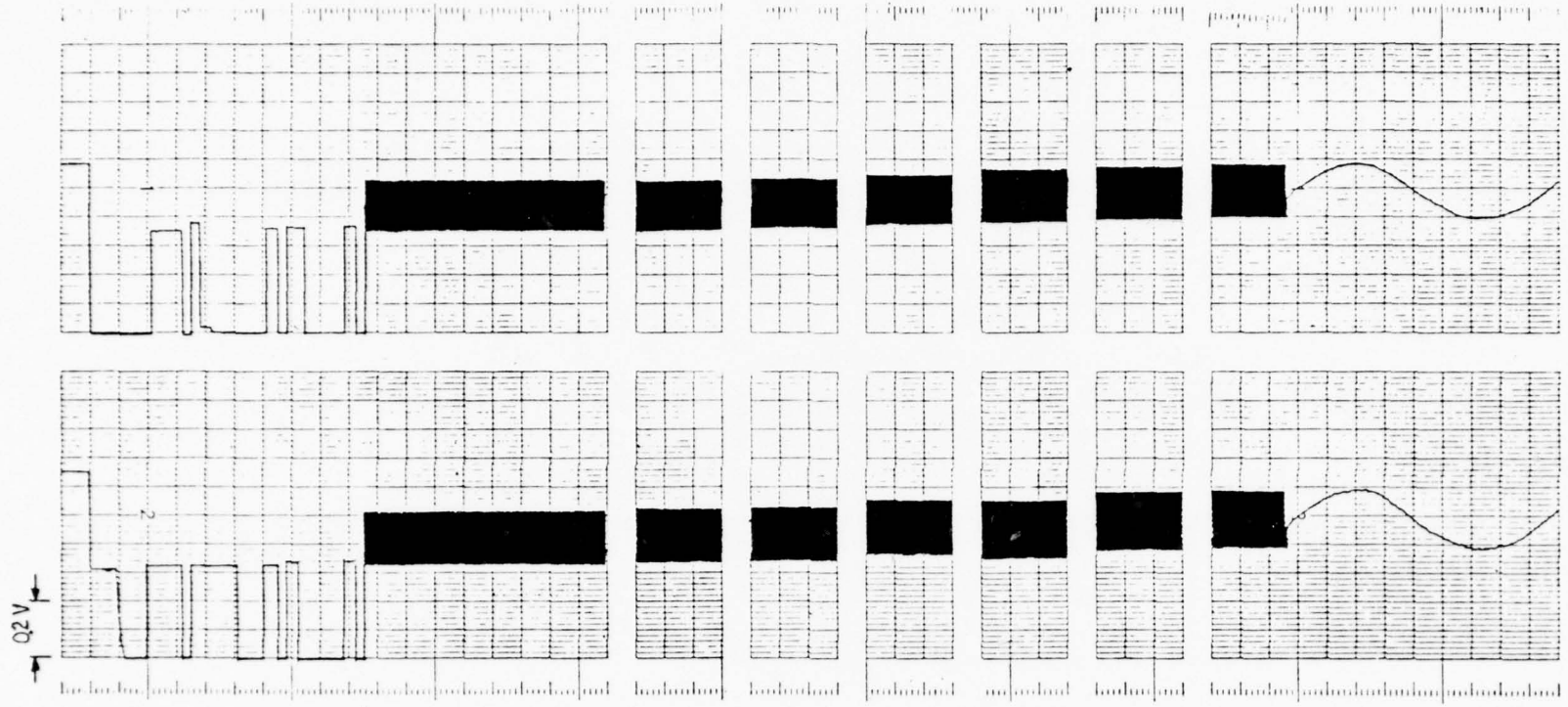

TIME	2:03	2:04	2:26	2:50	3:21	4:32	5:47	7:12
MEAN STRAIN(μIN/IN)	837	854	888	964	1092	1201	1277	1336
AMPLITUDE (μIN/IN)	770	774	757	765	761	829	820	829

STRESS LEVELS: 228 PSI ↔ 2280 PSI AT 3Hz

TEST CONDITION: 176°F/95% R.H.

FIGURE 19. FATIGUE AND RELATED CREEP OF A 90° SPECIMEN TESTED AT 176°F/95% R.H. ENVIRONMENT.

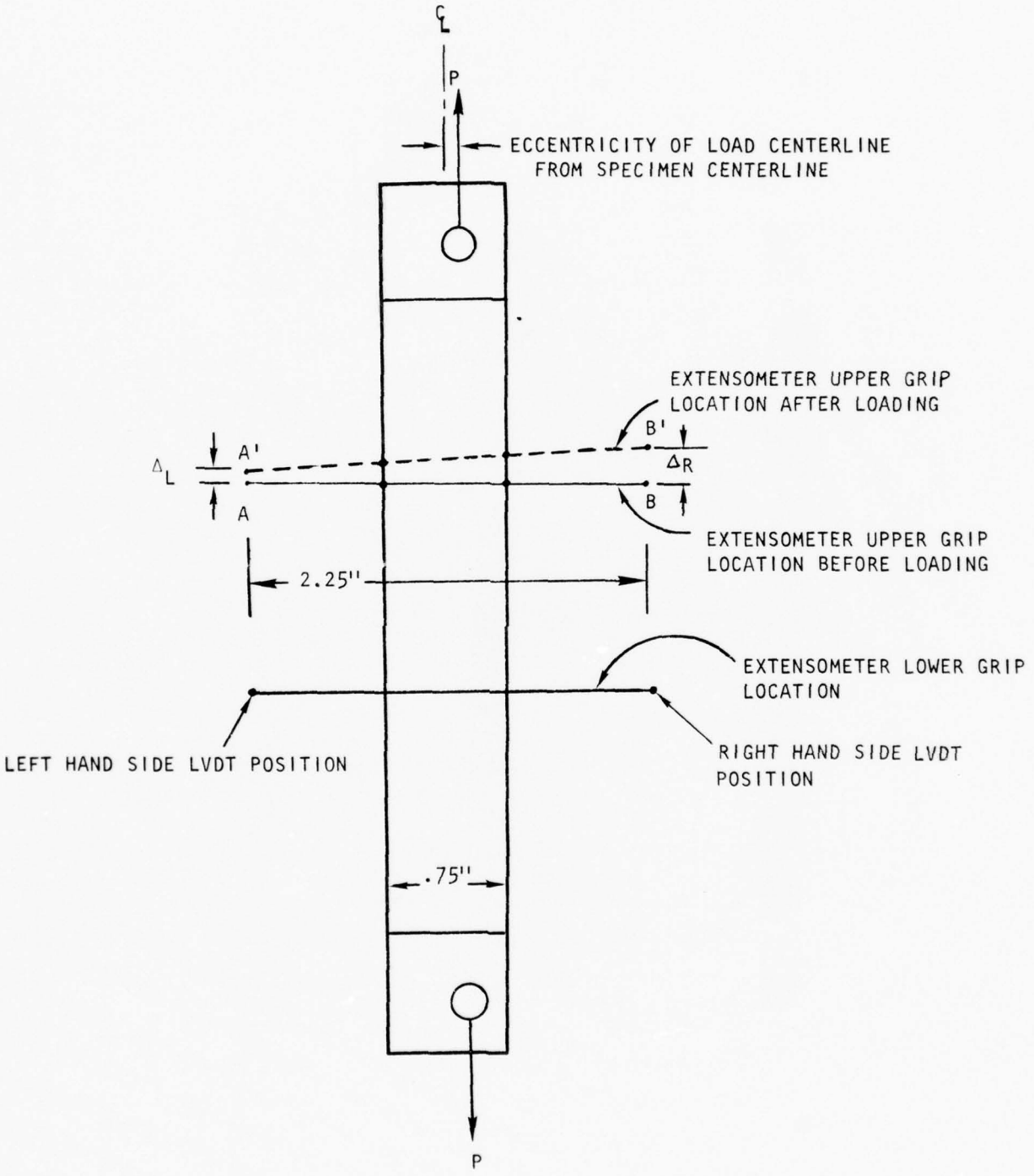

FIGURE 20. ECCENTRICITY AS SEEN BY EXTENSOMETER.

6.0 ANALYSIS OF CREEP-RECOVERY TEST RESULTS

6.1 DATA REDUCTION TECHNIQUE

The creep compliance, ε/σ, of AS/3501-6 material can be assumed to obey a power law relationship previously mentioned in section 4.1.

$$D = D(t, T, R.H.) = D_o + D_1 t^n$$

Since the net creep compliance $D - D_o$ is usually much smaller than the initial compliance, D_o, values D_o, D_1, and n of equation (2) can not be accurately found from short term creep test data only. However, a satisfactory data reduction technique was developed by Lou and Schapery[7] to evaluate the power law constants from creep and recovery test data such as is shown in Figure 21. In essence, if σ_o is the uniaxial creep stress applied to the specimen, $\varepsilon_r(t)$ is the recovery strain, and t_c is the time at which recovery begins, then for $t \to t_c$, we have

$$\frac{\varepsilon_r(t)}{\sigma_o} = (D_o + D_1 t^n) - [D_o + D_1 (t - t_c)^n]$$

$$= \Delta D(t_c)\,[(1 + \lambda)^n - \lambda^n] \qquad (11)$$

where $\Delta D(t_c) = D_1 t_c^n$ and $\lambda = (t - t_c)/t_c$

Equation (11) may be written in logarithmic form:

$$\log \varepsilon_r = \log \Delta D(t_c) + \log\,[(1 + \lambda)^n - \lambda^n] + \log \sigma_o \qquad (12)$$

By plotting $\log \varepsilon_r$ vs. $\log \lambda$ from recovery data shown in Figures 14 through 18 and comparing it with the $\log\,[(1 + \lambda)^n - \lambda^n]$ vs. $\log \lambda$ curve, the appropriate exponent n can be determined. Linear regression techniques can then be used to evaluate D_o and D_1 from the creep test data. Following this procedure, it was determined that $n = 0.18$, as shown in Figure 22, is an appropriate value for AS/3501-6 material in all environments. The exponent n was found to be a constant, independent of time, temperature, humidity and stress level. The D_o and D_1 values, as evaluated from test results, are shown in Tables 4 through 6.

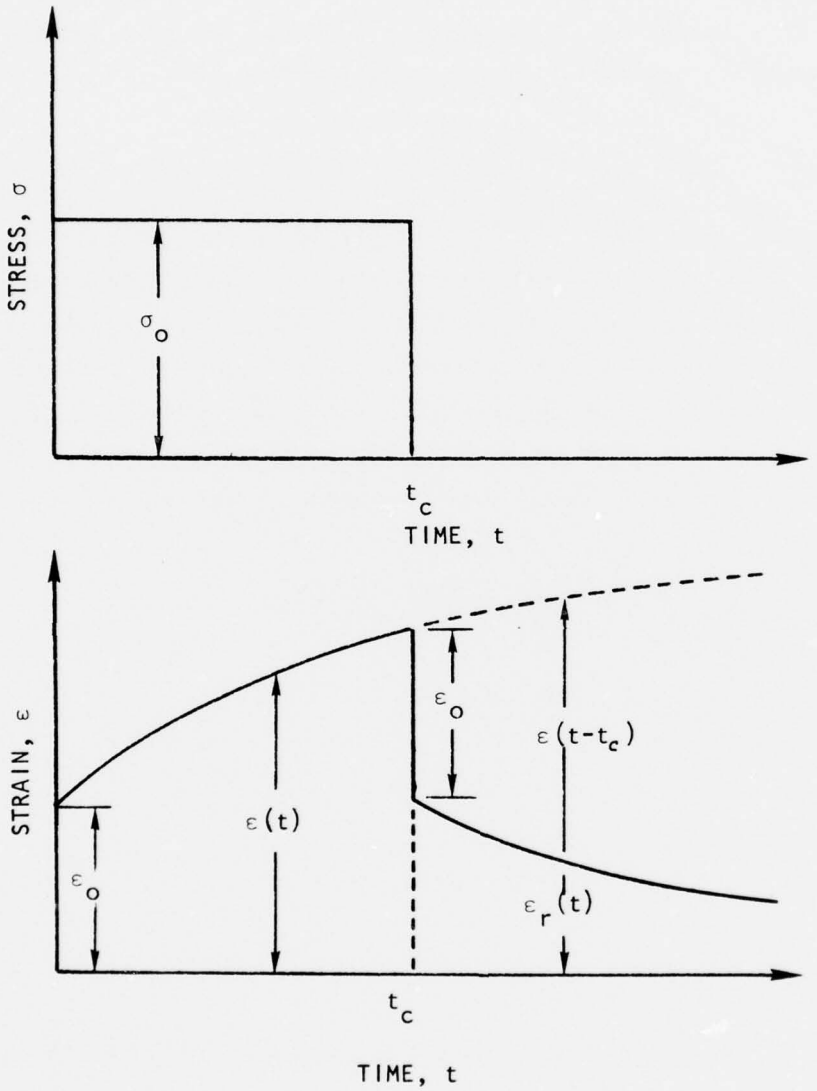

FIGURE 21. RELATION BETWEEN CREEP AND RECOVERY OF A LINEAR VISCOELASTIC MATERIAL.

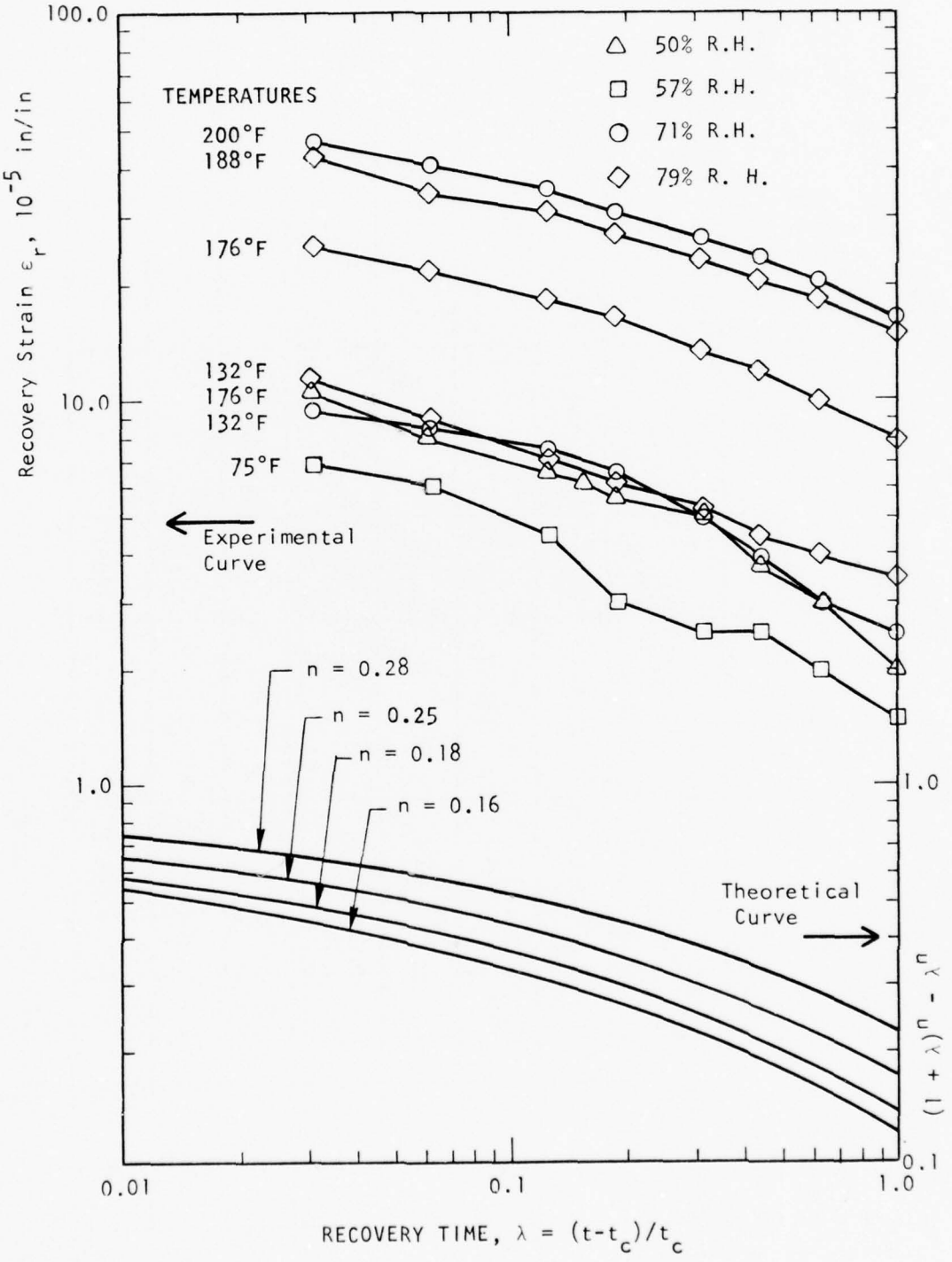

FIGURE 22. CURVE FITTING TECHNIQUE FOR POWER LAW EXPONENT

TABLE 4. POWER LAW CONSTANTS FROM CREEP-RECOVERY TEST OF ±45° SPECIMEN.

TEST ENVIRONMENT		STRESS LEVEL KSI	D_o (10^{-7} PSI^{-1})	D_1 (10^{-7} PSI^{-1})	LOG a_T	SPECIMEN ID	COMMENTS
TEMP. (°F)	HUMIDITY (% R.H.)						
75	50	4.945	3.412	.108	0	45-75-0-50	--
132	"	"	3.558	.181	-1.246	"	--
158	"	"	3.687	.285	-2.341	"	--
176	"	"	3.759	.397	-3.141	"	--
75	57	5.171	3.441	.143	0	45-200-57-30	--
132	"	"	3.677	.211	-.939	"	--
176	"	"	4.094	.341	-2.097	"	--

TABLE 5. POWER LAW CONSTANTS FROM CREEP-RECOVERY TEST OF ±45° SPECIMEN.

TEST ENVIRONMENT		STRESS LEVEL KSI	D_o (10^{-7} PSI^{-1})	D_1 (10^{-7} PSI^{-1})	LOG a_T	SPECIMEN ID	COMMENTS
TEMP. (°F)	HUMIDITY (% R.H.)						
75	71	4.938	3.606	.212	0	45-200-71-63	--
132	"	"	3.858	.317	-.971	"	--
158	"	"	4.069	.537	-2.242	"	--
176	"	"	4.131	.787	-3.165	"	--
200	"	"	4.019	1.060	-.3883	"	--
75	79	4.893	3.665	.220	0	45-200-79-65	--
132	"	"	3.945	.341	-1.057	"	--
158	"	"	4.097	.532	-2.131	"	--
176	"	"	4.166	.774	-3.035	"	--
188	"	"	4.093	1.181	-4.055	"	--

TABLE 6. POWER LAW CONSTANTS FROM CREEP-RECOVERY TEST OF 90° SPECIMEN.

TEST ENVIRONMENT		STRESS LEVEL KSI	D_o (10^{-7} PSI^{-1})	D_1 (10^{-7} PSI^{-1})	LOG a_T	SPECIMEN ID	COMMENTS
TEMP. (°F)	HUMIDITY (% R.H.)						
75	50	1.370	6.099	.199	0	90-80-0-41	Minor Mechanical Disturbance Effected Test Data
132	"	"	6.712	.314	-1.100	"	"
200	"	"	7.001	.436	-1.892	"	"

The power law relation in equation (2) can be rewritten as

$$D = D_o + D_1' \, (t/a_{TH})^n \tag{13}$$

where D_1' is, by definition, a constant and is equal to D_1 at reference temperature and humidity. Comparing equations (2) and (13), we see that the shift factor, a_{TH}, becomes

$$a_{TH} = a(T, \text{ R.H.}) = (D_1'/D_1)^{1/n} \tag{14}$$

Among creep-recovery tests, we have seventeen environmental tests for ± 45° specimens and three 50% R.H. tests for 90° specimen. The creep-recovery results are obtained by uniaxial measurement from the extensometers. In order to characterize the shear modulus G_{12} from equation (10), it was necessary to have test data for transverse modulus E_{22} in the environments for which ± 45° specimens had been tested. Without resorting to complete testing of 0° and 90° specimens at all environments, the Halpin-Tsai equations, below, can be employed for characterization.

$$E_{22} = E_M \frac{[E_f(1 + \zeta_e V_f) + \zeta_e E_M(1 - V_f)]}{E_f(1 - V_f) + \zeta_e E_M \left(1 + \dfrac{V_f}{\zeta_e}\right)} \tag{15}$$

$$G_{12} = G_M \frac{[G_f(1 + \zeta_g V_f) + \zeta_g G_M(1 - V_f)]}{G_f(1 - V_f) + \zeta_g G_M \left(1 + \dfrac{V_f}{\zeta_g}\right)} \tag{16}$$

In essence, a test-analysis procedure is developed to characterize the composite. This procedure, shown in the flow chart, Figure 23, is based on the following two basic assumptions.

1. Halpin-Tsai equations are valid for composites, quasi-statically, at all environments if the matrix properties are obtained from tests of the composite materials.
2. Fiber mechanical quantities will not vary with respect to time, temperature, and humidity.

From Procedures I and II of Figure 23, fiber volume, V_f, major Poisson's ratio, ν_{12}, and longitudinal Young's modulus, E_{11}, can be evaluated. Here, the

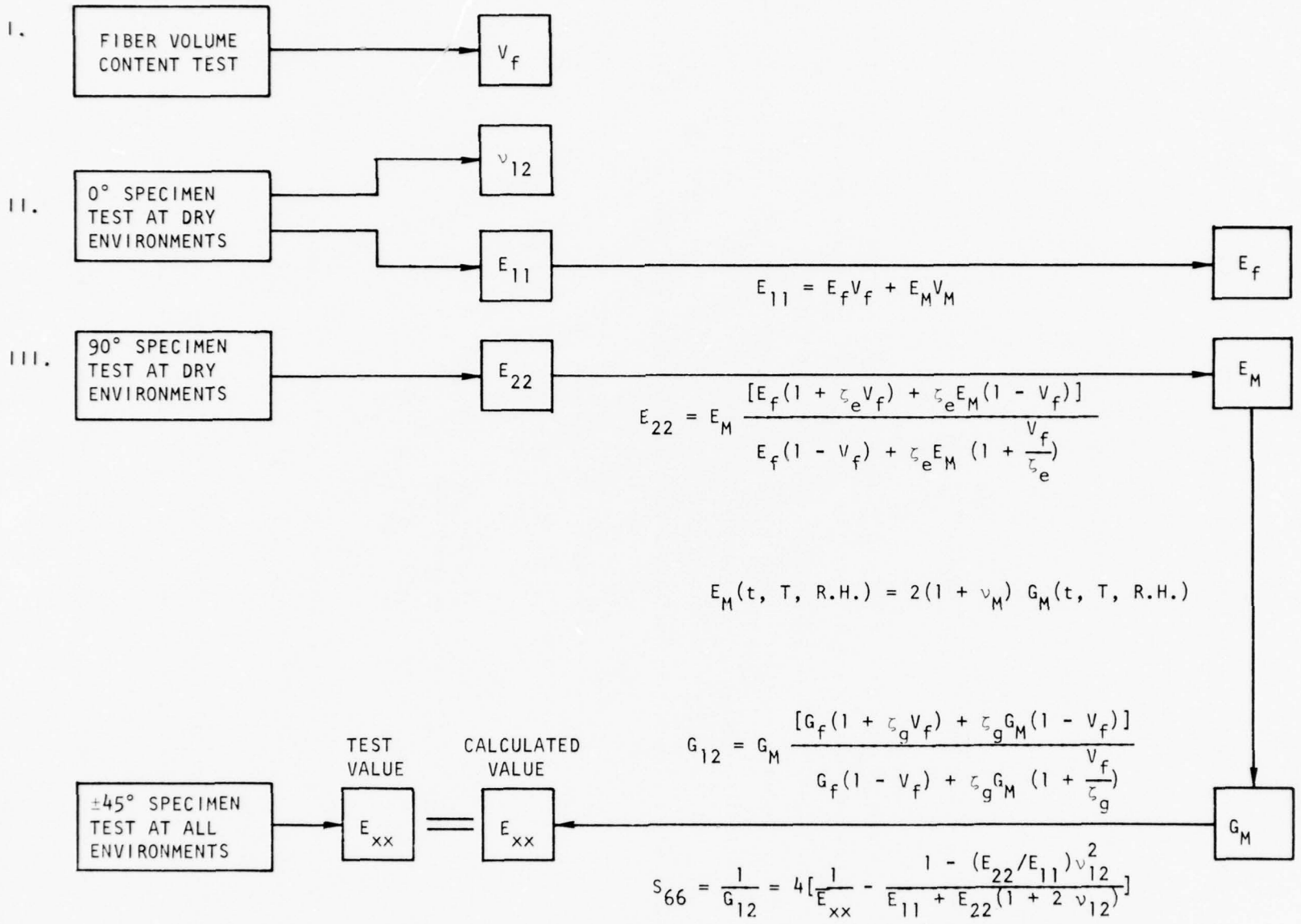

FIGURE 23. TEST-ANALYSIS PROCEDURE FOR THE CHARACTERIZATION OF COMPOSITE.

biaxial measurements in temperature-only environments for 0° specimens were obtained using strain gages. Fiber longitudinal modulus E_f can be found from the rule of mixtures. The results are listed in Table 7 including the theoretical relation assumed for later analysis purposes. Other than the four measured quantities just discussed (E_{11}, ν_{12}, V_f, and E_f), the ± 45° modulus E_{xx} depends on the parameters listed below.

$$E_{xx} = \bar{E}_{xx} (G_f, \nu_m, E_{22}, \zeta_e, \zeta_g) \tag{17}$$

The parameters in the argument are, respectively, fiber shear modulus, resin Poisson's ratio, composite transverse modulus, and geometric parameters in the Halpin-Tsai equations. Equation (17) is obtained from the Halpin-Tsai equations and equation (10). Transverse modulus E_{22}, instead of resin Young's modulus E_M, is used as an independent variable in equation (17), because a relationship between E_{xx} and E_{22} is more useful in relating analysis to test data.

Procedure III of Figure 23 is the algorithm to generate all other mechanical properties from known ± 45° and 90° test results based on equation (17). To start with the algorithm, four parameters, fiber shear modulus, G_f, matrix Poisson's ratio, ν_m, and geometry parameters ζ_e and ζ_g in the Halpin-Tsai equations, are assumed. For each test value E_{22}, a composite shear modulus, G_{12}, can be evaluated from the Halpin-Tsai equations and the ± 45° modulus, E_{xx}, can then be found from the functional relation (17). This calculated value, E_{xx}, should agree with the test value of E_{xx} if we have the correct parameters G_f, ν_m, ζ_e and ζ_g to begin with. A good initial assumption will expedite this algorithm exercise to determine realistic values for the four parameters. Various sources of information are collected here for this purpose.

(1) Fiber shear modulus, G_f, is assumed to be $4 \sim 10 \times 10^6$ psi in the literature[8,9] and Poisson's ratio, ν_m, varies from 0.35 to 0.41.[3,10]

(2) At low value of E_{22}, an approximate relation

$$(1 + \nu_m)(1 + \zeta_e V_f)/(1 + \zeta_g V_f) = 2\, E_{22}/E_{xx} \tag{18}$$

can be obtained through the Halpin-Tsai equations and equation (10). We also know that $\zeta_e = 2$ and $\zeta_g = 1$ are the values for the general composite with isotropic fiber. The matrix Poisson's ratio, ν_m, is

TABLE 7. MAJOR POISSON'S RATIO AND YOUNG'S MODULI OF AS/3501-6 MATERIAL AT VARIOUS TEMPERATURE LEVELS.

TEMPERATURE (°F)	MAJOR POISSON'S RATIO (ν_{12})	MAJOR YOUNG'S MODULUS (E_{11}, 10^6 PSI)	FIBER LONGITUDINAL MODULUS* (E_f, 10^6 PSI)
75	.346	18.97	30.60
132	.351	18.88	30.45
156	.350	18.93	30.53
200	.339	18.93	30.53
THEORETICAL ANALYSIS VALUE	.35	18.95	30.5

*FIBER LONGITUDINAL MODULUS IS CALCULATED FROM RULE OF MIXTURES AND THE FIBER VOLUME CONTENT IS ASSUMED TO BE 62%.

essentially constant as discussed in section 4.2. At a high value of E_{22}, the value E_{22}/E_{xx} seems increasing linearly with respect to E_{22} value.

(3) A sensitivity study of E_{xx} with respect to the four parameters G_f, ζ_e, ζ_g and ν_m will help to check the relative importance of the initially assumed magnitude of the four parameters. This is done by the sensitivity equation

$$\frac{\Delta E_{xx}}{E_{xx}} = \frac{\partial \ln E_{xx}}{\partial \ln G_f}\frac{\Delta G_f}{G_f} + \frac{\partial \ln E_{xx}}{\partial \ln \zeta_e}\frac{\Delta \zeta_e}{\zeta_e} +$$

$$\frac{\partial \ln E_{xx}}{\partial \ln \zeta_g}\frac{\Delta \zeta_g}{\zeta_g} + \frac{\partial \ln E_{xx}}{\partial \ln \nu_m}\frac{\Delta \nu_m}{\nu_m} + \frac{\partial \ln E_{xx}}{\partial \ln E_{22}}\frac{\Delta E_{22}}{E_{22}} \qquad (19)$$

where Δ means the difference between the true value and the assumed value.

These three statements were found to be very useful in pursuing the Procedure III algorithm. We assumed

$$G_f = 10 \times 10^6 \text{ psi}$$

$$\nu_m = .35 \qquad (20)$$

as our initial guess. From Tables 4 and 6, three initial values of the ratio E_{22}/E_{xx} were evaluated to be .559, .530, and .556 at temperatures 75°F, 132°F, and 200°F respectively. Since the left hand side of equation (18) is roughly a constant, a value 0.559 is assumed for the ratio E_{22}/E_{xx} by using the fact that room temperature data are more reliable than that of other environments. Even with known values for ν_m and E_{22}/E_{xx}, numerous choices of the parameters ζ_e and ζ_g can be fitted into equation (18). We started with $\zeta_e = 2$ as we did for the isotropic fiber composite and varied the ζ_g value around 2.75 which was obtained from approximation equation (18). It seems that $\zeta_g = 3.7$ gives the best fit of experimental data as shown in Figure 24 which is obtained by inserting various values of E_{22} in equation (17) according to the Procedure III algorithm.

Before adjusting the initial value of the parameters selected for the second exercise in Procedure III, we differentiated equations (10), (15) and (16) with respect to G_g, ζ_e, ζ_g and ν_m and substituted in the assumed parametric values, the sensitivity equation (19) could then be evaluated as

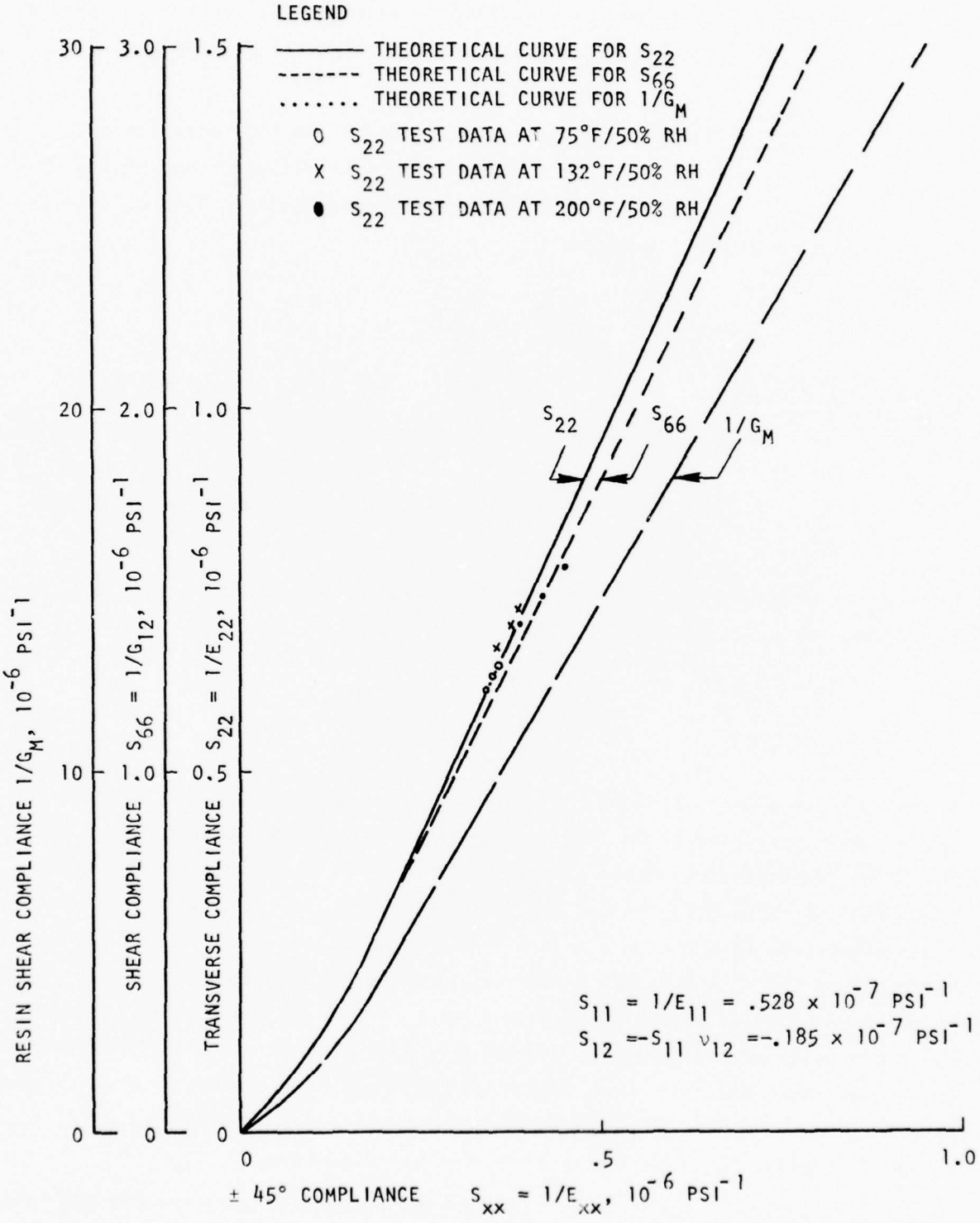

FIGURE 24. NOMOGRAPH OF TEST-ANALYSIS FOR COMPOSITE PROPERTIES.

$$\left.\frac{\Delta E_{xx}}{E_{xx}}\right| = .0805\,\frac{\Delta G_f}{G_f} + .5425\,\frac{\Delta \zeta_g}{\zeta_g} - .4332\,\frac{\Delta \zeta_e}{\zeta_e} - .2075\,\frac{\Delta \nu_m}{\nu_m} + .8581\,\frac{\Delta E_{22}}{E_{22}}$$

$$E_{22} = 1.4 \times 10^6$$

$$\left.\frac{\Delta E_{xx}}{E_{xx}}\right| = .0090\,\frac{\Delta G_f}{G_f} + .1787\,\frac{\Delta \zeta_g}{\zeta_g} - .1423\,\frac{\Sigma \zeta_e}{\zeta_e} - .0672\,\frac{\Delta \nu_m}{\nu_m} + .2645\,\frac{\Delta E_{22}}{E_{22}} \qquad (21)$$

$$E_{22} = 0.5 \times 10^6$$

This result indicates that E_{xx} is a weak function of G_f and ν_m as far as their variation ranges are concerned. If the approximate relation (18) is introduced in equation (21), we have

$$\left.\frac{\Delta E_{xx}}{E_{xx}}\right| = .0805\,\frac{\Delta G_f}{G_f} + .0010\,\frac{\Delta \zeta_g}{\zeta_g} - .2075\,\frac{\Delta \nu_m}{\nu_m} + .8581\,\frac{\Delta E_{22}}{E_{22}}$$

$$E_{22} = 1.4 \times 10^6$$

$$\left.\frac{\Delta E_{xx}}{E_{xx}}\right| = .0090\,\frac{\Delta G_f}{G_f} + .0008\,\frac{\Delta \zeta_g}{\zeta_g} - .0672\,\frac{\Delta \nu_m}{\nu_m} + .2645\,\frac{\Delta E_{22}}{E_{22}} \qquad (22)$$

$$E_{22} = 0.5 \times 10^6$$

Thus, E_{xx} is a weak function of ζ_g (or ζ_e) if the approximate equation (18) is strictly followed. Other combinations of G_f, ζ_e and ν_m data were tried and a better fit was not obtained between theoretical and experimental data. We can only expect the E_{xx} value to be most sensitive to E_{22} according to equation (22). It is also interesting to note that the value E_{22}/E_{xx} is almost linear with respect to E_{22} as shown in Figure 25 which is a side result obtained from Procedure III. We have also shown, in Figure 24, the relations of in-situ resin shear modulus as related to E_{xx}.

By using Figure 24 and Tables 4 and 5, compliances S_{22} and S_{66} are readily determined. This together with the analysis in Section 4.1, can completely characterize all compliances S_{ij} at all seventeen environments.

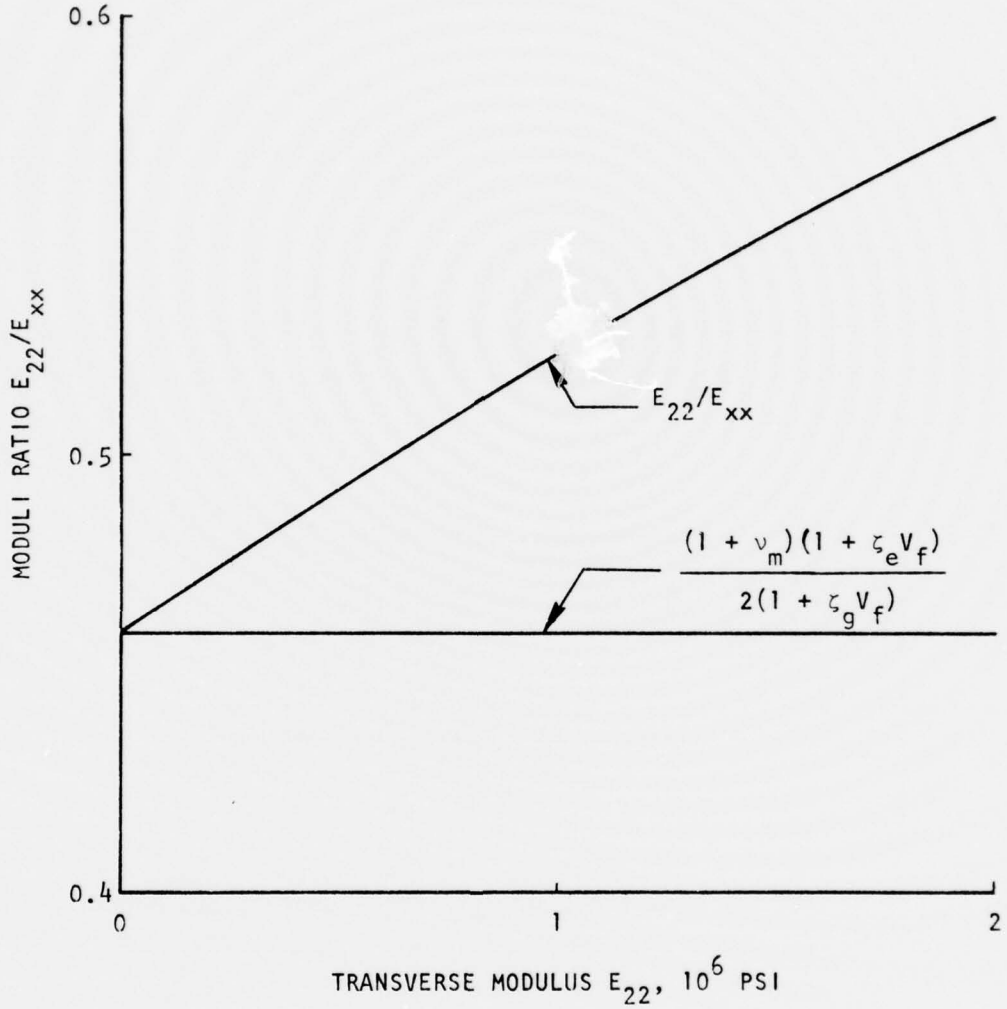

FIGURE 25. COMPARISON OF TRUE VALUE AND APPROXIMATE VALUE OF THE RATIO E_{22}/E_{xx} VS. E_{22}.

The above discussions can be summarized by showing an example. Suppose we are interested in the behavior of the shear compliance $S_{66} = 1/G_{12}$ in an 132°F/71% R.H. environment. We start from Table 5 where we find that $D_o = .3858 \times 10^{-6}$ psi^{-1} and $D_1 = .0317 \times 10^{-6}$ psi^{-1}. So, the power law representation for a ±45° laminate at 132°F/71% R.H. environment is

$$S_{xx} = (.3858 + .0317\ t^{.18}) \times 10^{-6}\ psi^{-1}$$

By inserting various values of t in the equation above, we find the corresponding S_{xx} values and, by using Figure 24, we find the corresponding S_{66} values. Thus, we have the table

t	S_{xx}	S_{66}
0	.3858	1.38
1	.4175	1.50
100	.4584	1.66

By evaluating the coefficients D_o and D_1 for S_{66} from the Table above, the power law representation for S_{66} can be approximated as

$$S_{66} = (1.38 + .12\ t^{.18}) \times 10^{-6}$$

at environment 130°F/71% R.H. Following the procedure in the example above, we can find power law representation for S_{22}, $1/E_M$ or $1/G_M$ by using Tables 4 or 5 and Figure 24.

6.2 TEMPERATURE AND HUMIDITY EFFECT AND MASTER CURVES

For analysis purposes, test data D_o, D_1, and log a_T in Tables 4 through 5 are plotted in Figures 26 through 30. The shift factor, a_T, is normalized to unity at 75°F for each relative humidity level. From the discussion of the previous section, we are able to determine the power law equations (13) and (14) to characterize the compliances S_{ij}. The temperature and humidity effect on the net creep compliances $\Delta D = D - D_o$ is experienced through the shift factor a(T, R.H.).

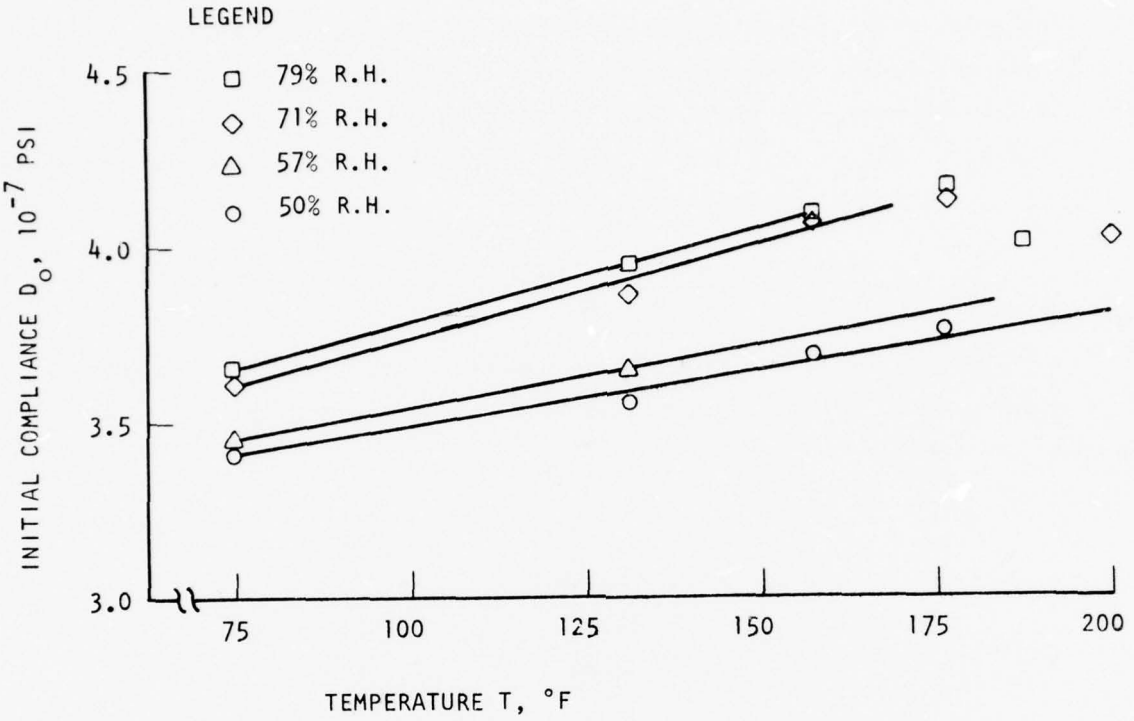

FIGURE 26. TEMPERATURE DEPENDENCE OF INITIAL COMPLIANCE D_o AT VARIOUS HUMIDITY LEVELS.

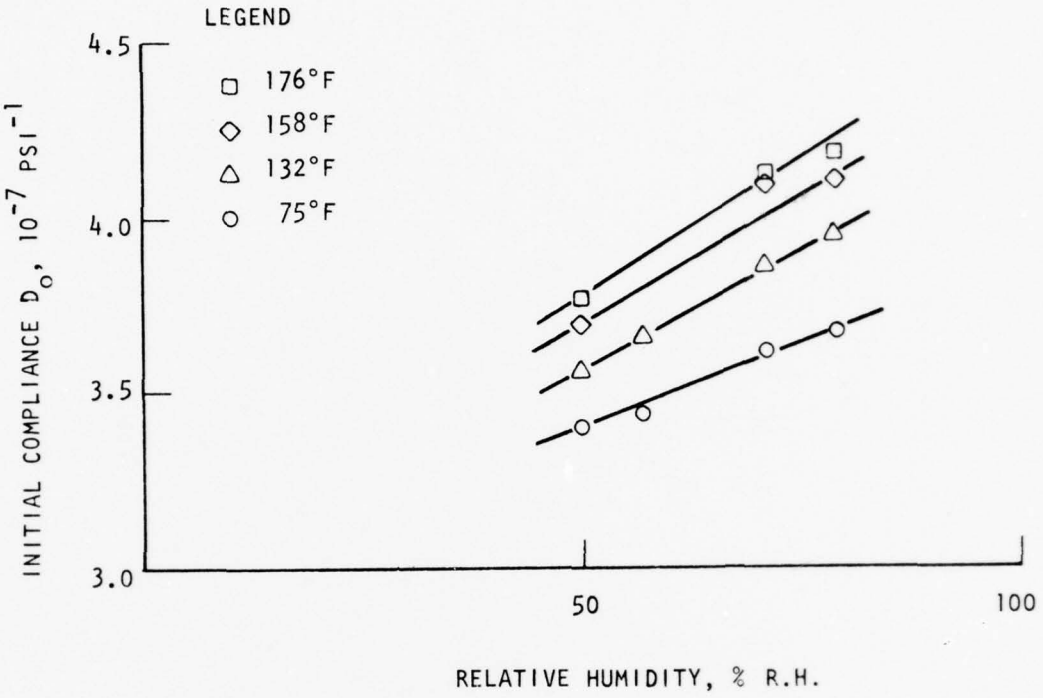

FIGURE 27. HUMIDITY DEPENDENCE OF INITIAL COMPLIANCE D_o AT VARIOUS TEMPERATURE LEVELS.

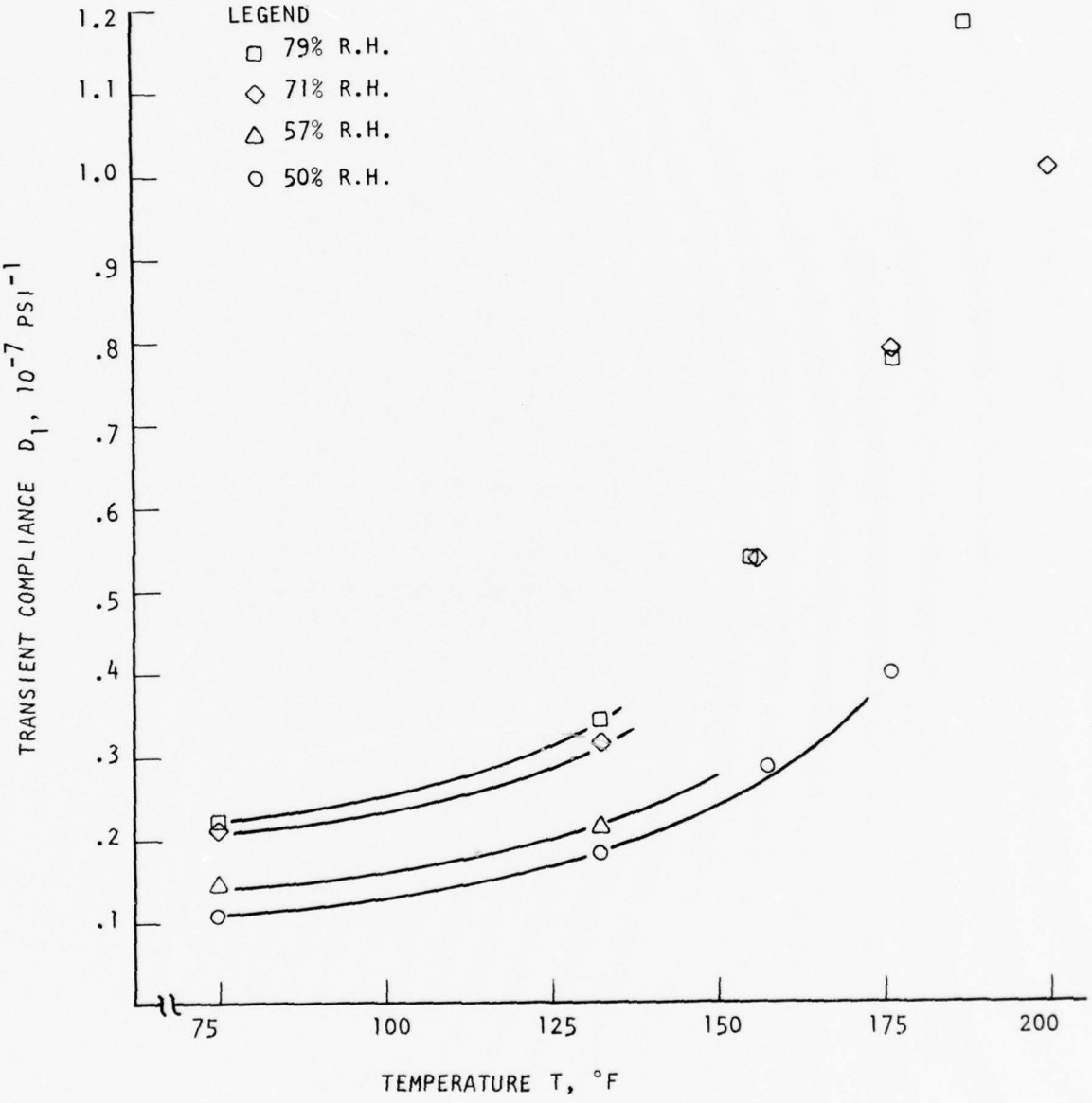

FIGURE 28. TEMPERATURE DEPENDENCE OF TRANSIENT CREEP COMPLIANCE D_1 AT VARIOUS HUMIDITY LEVELS.

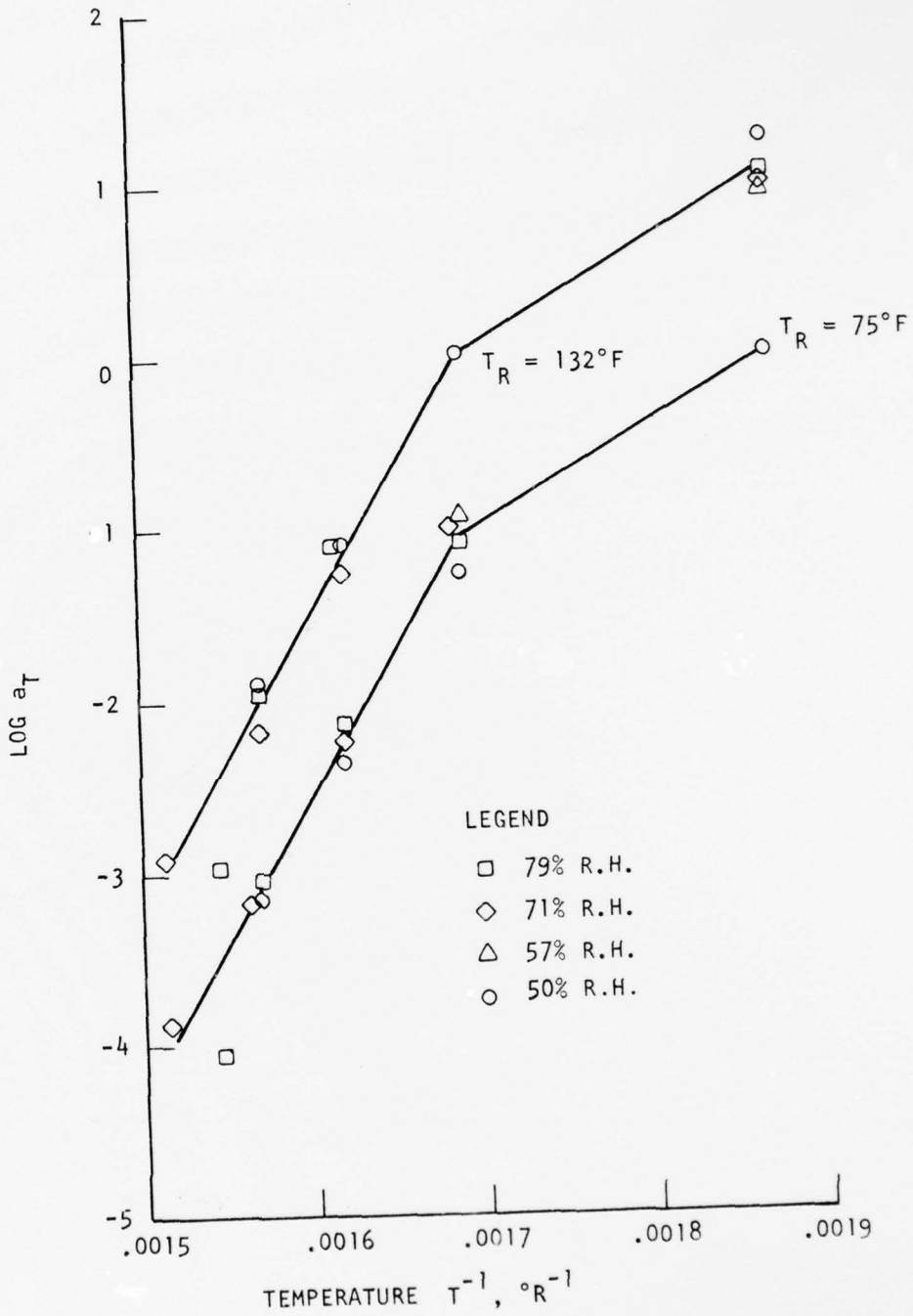

FIGURE 29. TIME-TEMPERATURE SHIFT FACTOR a_T for MOISTURE SATURATED COMPOSITES.

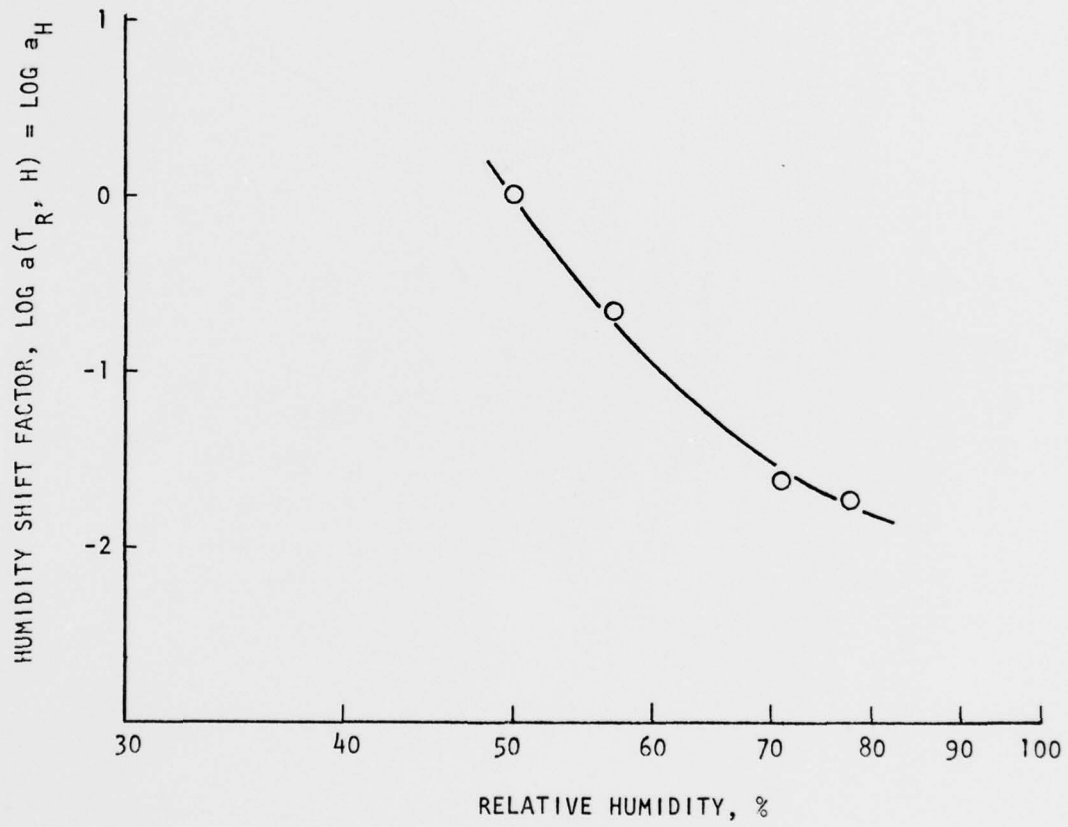

FIGURE 30. TIME-HUMIDITY SHIFT FACTOR $a(T_R, H)$ FOR MOISTURE SATURATED COMPOSITE (T_R = 75°F).

Test results in Figure 29 indicate an interesting phenomenon of our shift factor, a_T, i.e., humidity does not affect significantly the log a_T value at each temperature level. This implies that a(T, R.H.) is a function of temperature and humidity in a product form

$$a(T, R.H.) = a_T(T_R, R.H.) = a_T\, a_H \tag{23}$$

and Figure 29 is the characteristic curve for a_T only. The term a_H is found by evaluating a(T, R,H,) at reference temperature T_R = 75°F (Figure 30) and will be referred to as the humidity shift factor. Equation (23) and Figures 29 and 30 represent the equivalence in temperature effect and humidity effect on AS/3501-6 composite in that their shift factors, a_T and a_H, become additive in the logarithmic scale.

Assuming the straight lines in Figures 26 and 27 are good approximations of test results in the temperature and humidity range we have tested so far, the initial compliance D_o will have the form of a linear combination of temperature T (°F) and relative humidity, H (% R.H.)

$$D_o = aTH + bT + CH + d \tag{24}$$

The master curve of net creep compliance $\Delta D = D - D_o$ for $D_{xx} \approx 1/E_{xx}$ can be obtained by shifting data in the log t scale, with respect to both temperature and humidity data in Figures 29 and 30 and the result is shown in Figure 31. The experimental data agree with the master curve reasonably well. For values of S_{xx} greater than 0.25×10^{-6} psi^{-1}, the curves in Figure 24 are essentially straight lines. This means that values S_{22}, S_{66} and $1/G_M$ can be linearly related to S_{xx} and they can be represented by the following power law equation based on equations (23), (13) and (24)

$$D = aTH + bT + CH + d + D_1' \left(\frac{t}{a_T\, a_H}\right)^{0.18} \tag{25}$$

where the constants a, b, c, and D_1' are listed in Table 8. Where S_{11} and S_{22} values are from inserts in Figure 24. The constants a, b and c were obtained by linear regression technique in Reference 11 and test data in Tables 4 and 5. Hence, mechanical characterization of AS/3501-6 composites has been defined between the temperature/humidity parameters of 75°F/50% R.H. and 200°F/95% R.H. They are completely defined by equation (25) together with Figures 29 and 30 and Table 8.

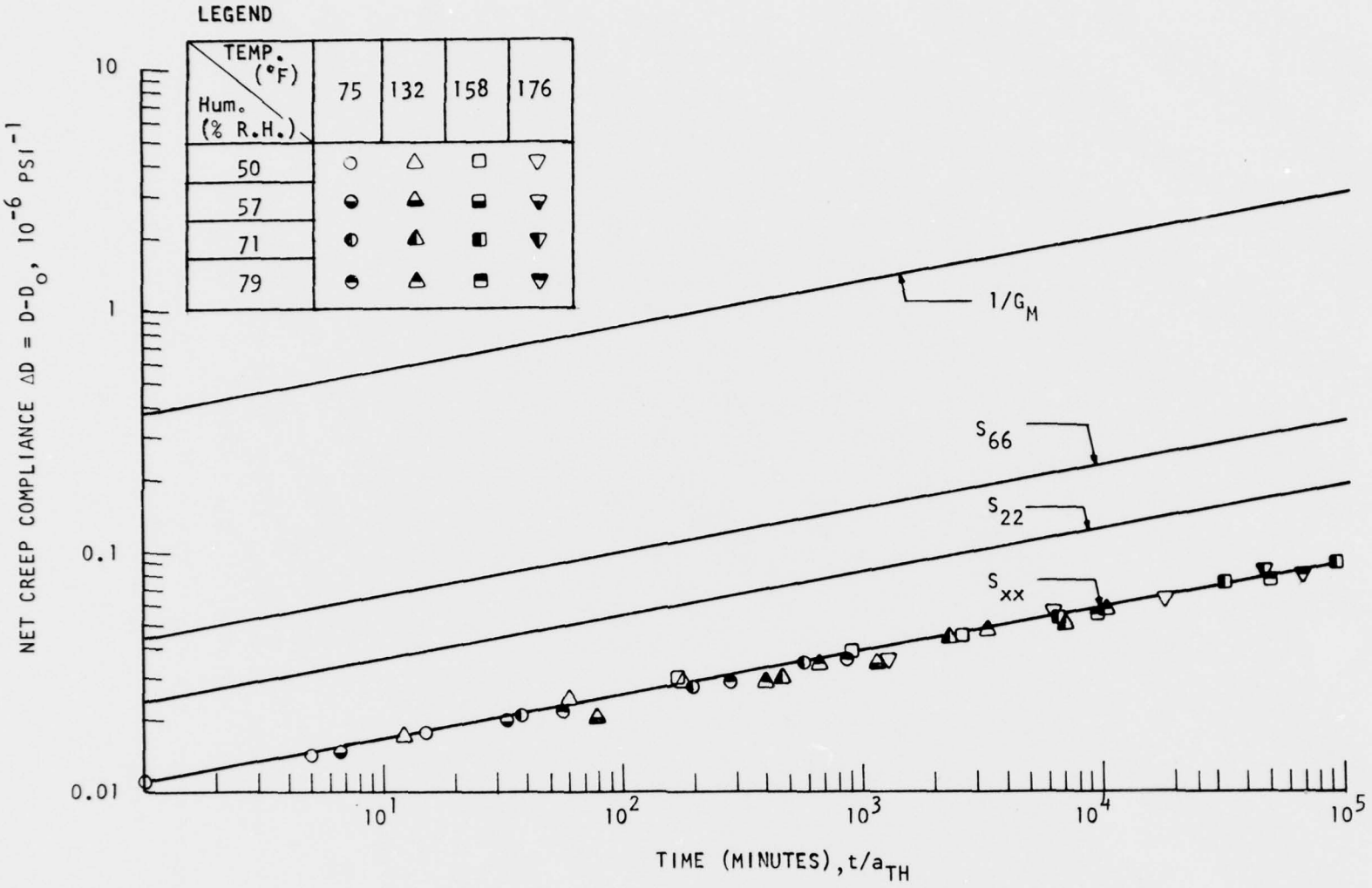

FIGURE 31. MASTER CURVES FOR NET CREEP COMPLIANCES.

TABLE 8. POWER LAW CONSTANTS FOR COMPLIANCES S_{ij} OF AS/3501-6 GR/EP COMPOSITE.

D^*	a 10^7(PSIx°FxRH)	b 10^{-7}(PSIx°F)$^{-1}$	c 10^{-7}(PSIxRH)$^{-1}$	d (10^{-7} PSI^{-1})	D_1' (10^{-7} PSI^{-1})
S_{xx}	0.00002263	0.002486	0.009196	2.6570	.108
S_{11}	0	0	0	0.5277	0
S_{12}	0	0	0	-0.1847	0
S_{22}	0.00004933	0.005419	0.020047	4.4823	.235
S_{66}	0.00009052	0.009944	0.036784	8.8280	.432

$^*D = aTH + bT + CH + d + D_1' \left(\frac{t}{a_T\, a_H}\right)^{0.18}$

From equation (25), we see that temperature and humidity effect composite compliance through D_o linearly and through D_1 logarithmically. Hence, the equivalence between temperature and humidity on composite compliance is through the relationship of equation (25) in a complicated way. Direct relationship between them will be feasible if the appropriate functional representations of shift factors a_T and a_H can be formulated from Figures 29 and 30. More environments need to be selected for $\pm 45°$ specimen testing to generate the smooth log a_T and log a_H curves so that the appropriate functional representations can be obtained.

7.0 ANALYSIS OF FATIGUE TEST RESULTS

The 90° specimens used for fatigue testing have the same configuration as those for static testing. The specimen dimensions are shown in Figure 1. Since the specimens were scheduled to be under pin-loading type fatigue in the Shore Western environmental test machine, end tabs of the specimens were sealed by RTV rubber to protect them from moisture penetration through environmental conditioning. This will ensure that the fatigure failure will occur in the gage section. Half of the fatigue specimens were tested with the thermocouple attached to the center gage area of the specimen during fatigue. The other half were monitored by the extensometer to study its creep and eccentricity during fatigue.

A total of thirty-one specimens that were saturated at 95% relative humidity were fatigued and the results are shown in Table 9. Most specimens were allowed to fatigue up to four hours at three Hertz frequency. Specimens that did not fail in fatigue were failed statically.

Although Table 9 does not show enough data for statistical fatigue analysis, it does show three interesting phenomena:

a. Three failure modes were observed: (1) failure in the end tab edge area, (2) failure at the gage section, and (3) failure at the pin load hole section. The first two failure modes dominate the fatigue failure.

b. Residual fatigue stress is always higher than the ultimate static tensile strength of 3,000 psi regardless of the environment and stress level used. (comparing Tables 1 and 9).

c. No surface temperature rise in the fatigue specimen was observed at the three Hertz frequency.

TABLE 9. FATIGUE TEST RESULTS FOR 90° SPECIMEN.

SPECIMEN ID	TEST ENVIRONMENT		STRESS LEVEL (% °F UTS)	CYCLES	STATIC RESIDUAL STRENGTH (PSI)	FAILURE MODE		
	TEMP. (°F)	HUMIDITY (% R.H.)				EDGE	GAGE	HOLE
90-200-95-92	132	95	70	43,400	4,145	X		
-93	"	"	"	43,660	3,779		X	
-98	"	"	"	5,230	-		X	
-99	"	"	"	5.170	-		X	
-94	"	"	"	43,000	4,165		X	
-95	"	"	"	43,000	4,829		X	
-80	"	"	"	42,700	5,126		X	
-82	"	"	"	42,400	3,794	X		
-81	"	"	"	43,200	5,137		X	
-86	"	"	"	43,200	4,799		X	
-78	"	"	"	468,650	-	X		
90-200-85-105	132	95	80	140	-		X	
-83	"	"		5,800	-		X	
-58	"	"		10,260	-	X		
-84	"	"		4,220	-		X	
-90	"	"		545	-	X		
-91	"	"		45,300	4,786		X	
-96	"	"		2,820	-	X		
-76	"	"		42,600	3,764	X		
-7	"	"		10,400	-	X		
-11	"	"		340	-	X		

TABLE 9. FATIGUE TEST RESULTS FOR 90° SPECIMEN. (CONTINUED)

SPECIMEN ID	TEST ENVIRONMENT		STRESS LEVEL (% °F UTS)	CYCLES	STATIC RESIDUAL STRENGTH (PSI)	FAILURE MODE		
	TEMP. (°F)	HUMIDITY (% R.H.)				EDGE	GAGE	HOLE
90-200-95-70	176	95	80	72,900	-		X	
-75	"	"	"	34,200	-			X
-79	"	"	"	12,300	-			X
-88	"	"	"	19,800	-		X	
-100	"	"	"	2,850	-	X		
-71	"	"	"	1,500	-		X	
-101	"	"	"	5,040	-	X		
90-200-95-72	200	95	80	1,800	-			X
-73	"	"	"	2,320	-	X		
-74	"	"	"	970	-			X

8.0 APPLICATION TO SKIN/SPAR DESIGN

8.1 BACKGROUND

Since temperature and humidity have a potentially detrimental effect on the mechanical performance of composite structure, a design example is presented to quantify the impact that the linear viscoelastic characteristics of AS/3501-6 graphite epoxy have on a typical design. A skin/spar joint design for a hybrid (composite/metal) wingbox is used as the design example. The typical cross-section of the wingbox is shown in Figure 32.

The element specimen design in Figure 35 shows the lower portion of the skin/spar design and is used here for analysis. The critical load condition of the joint is the fuel pressure pull-off condition. The ultimate pull-off design load is 1000 lbs.

The environmental design criteria used for the design was that the external surface temperatures for the joint area were to be a minimum of -80°F (-62°F) a maximum of 273°F (134°C)(10 minutes or less per exposure) and a maximum endurance temperature of 160°F (71°C). The worst humidity to be experienced was 75% R.H. for the outer skin area.

8.2 ELASTIC AND VISCOELASTIC ANALYSIS

The skin/spar design presents an interesting design problem in that the thickness direction of the skin has matrix dominant properties and is susceptible to structural failure. A finite element NASTRAN model was made to investigate this structural problem under severe environment. Two environments, 75°F/50% R.H. and 176°F/71% R.H., were selected for the study. The basic mechanical properties of the composite at these two environments are given in Table 10 and were obtained from Table 8 and equation (25). The properties at 75°F/50% R.H. were evaluated at zero creep time (instantaneous response) and that at 176°F/71% R.H. were at a one hour creep time which was to simulate the one hour mission flight.

The critically stresses area, based on NASTRAN model analysis, was located at the middle of the composite skin and around the skin-adhesive interface area, marked "A" in Figure 32. Interlaminar tension stress and

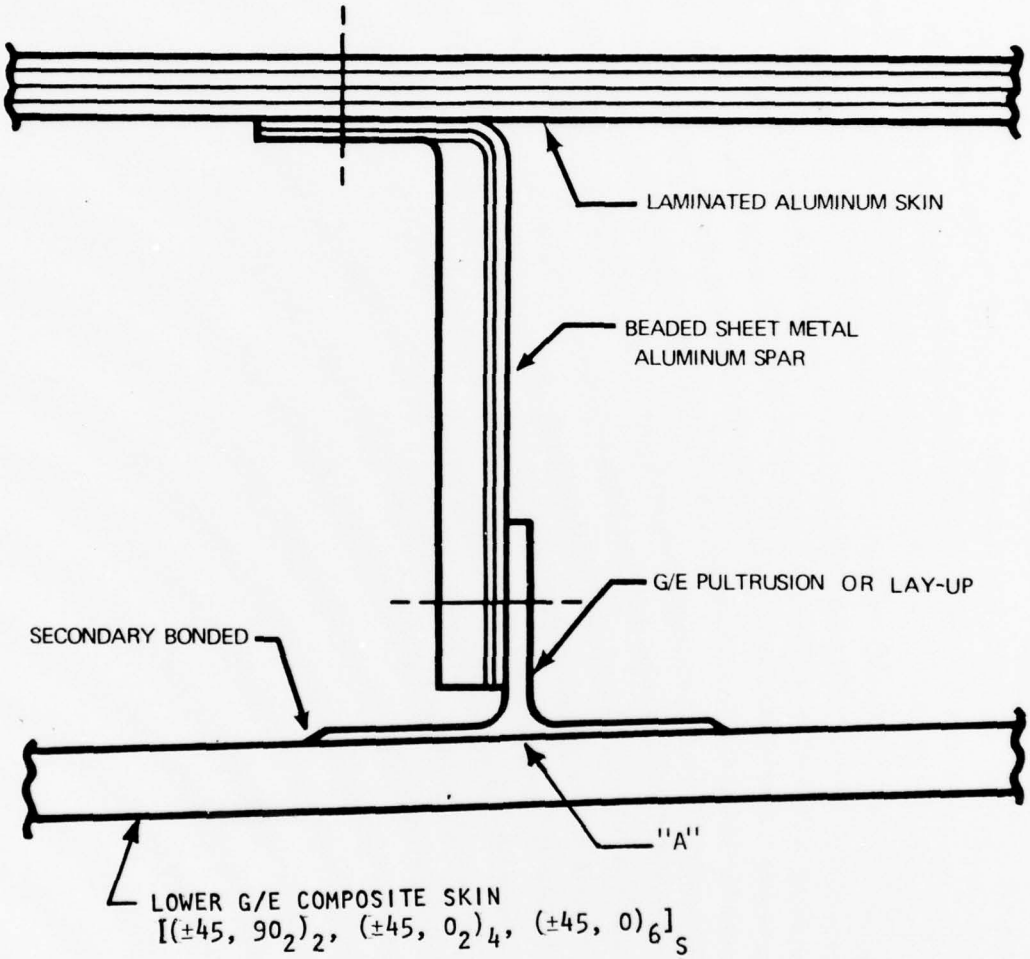

FIGURE 32. THE INTEGRATED SKIN/SPAR DESIGN.

chordwise tension stress in area "A", as shown in Figure 33 increased as the environment became more severe. The margin of safety (M.S.) is reduced to 0.63 at 176°F/71% R.H. from 2.93 at 75°F/50% R.H. Skin/Spar pull-off specimens were fabricated and tested to validate the analysis and the design. Failed specimens are shown in Figures 34 and 35. The failure mode and failure location agree very well with the analysis. Various modified skin/spar designs are now under evaluation internally to improve the interlaminar tensile strength.

TABLE 10. BASIC MECHANICAL PROPERTIES FOR SKIN/SPAR DESIGN.

	75°F/50% R.H.	176°F/71% R.H.
E_{11}	18.95×10^6 PSI	18.95×10^6 PSI
E_{22}	1.65×10^6 PSI	0.9×10^6 PSI
ν_{12}	0.35	0.35
G_{12}	$.85 \times 10^6$ PSI	$.47 \times 10^6$ PSI
Ultimate Strength in Transverse Direction	6,400 PSI	3,000 PSI
STRESS AT "A" FROM ANALYSIS:		
Chordwise Tension	6,300 PSI	7,300 PSI
Interlaminar Tension	1,600 PSI	2,100 PSI

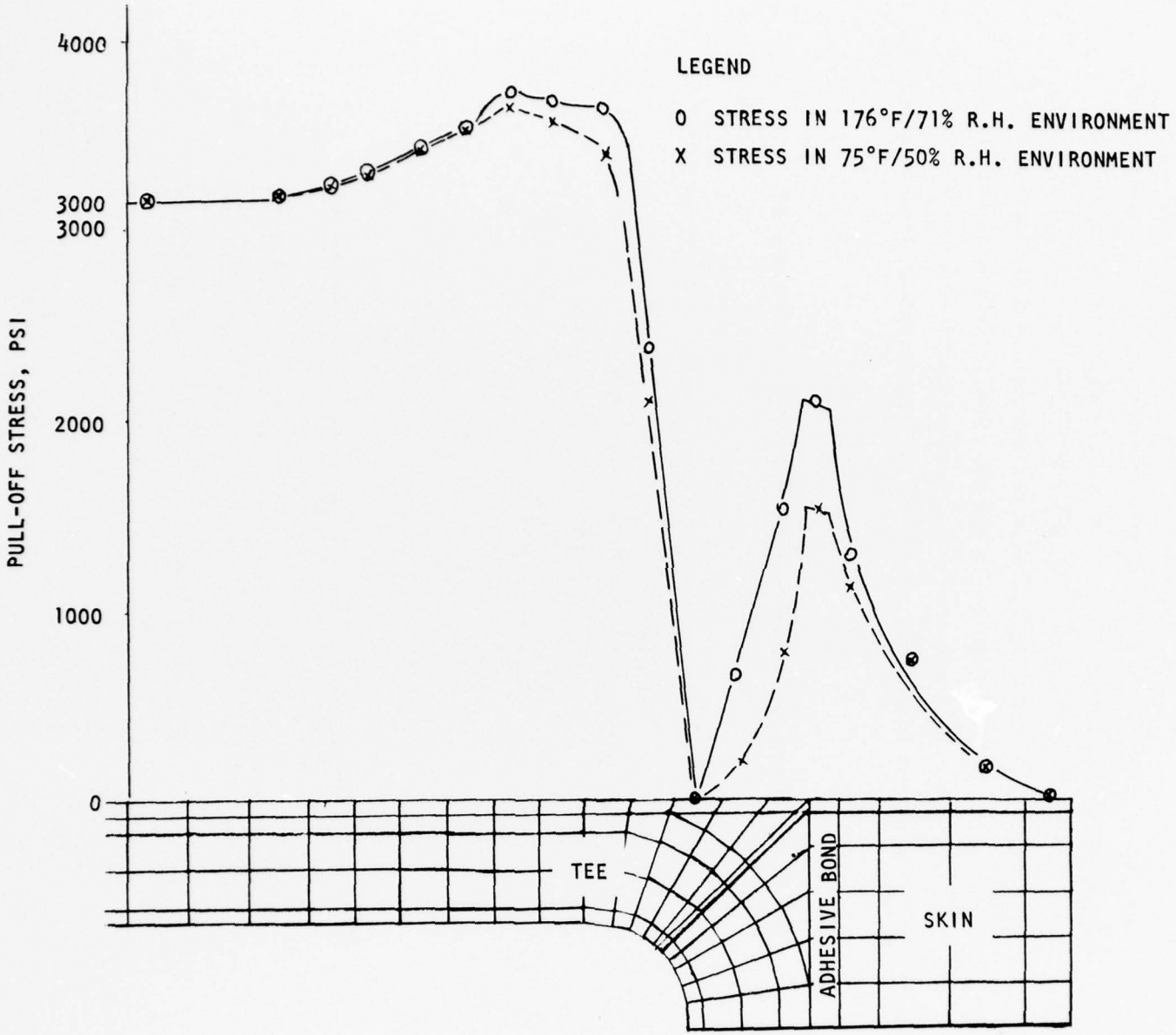

FIGURE 33. INTERLAMINAR NORMAL STRESS AT THE CENTER SECTION OF THE PULL-OFF SPECIMEN UNDER 1000 LB. PULL-OFF LOAD.

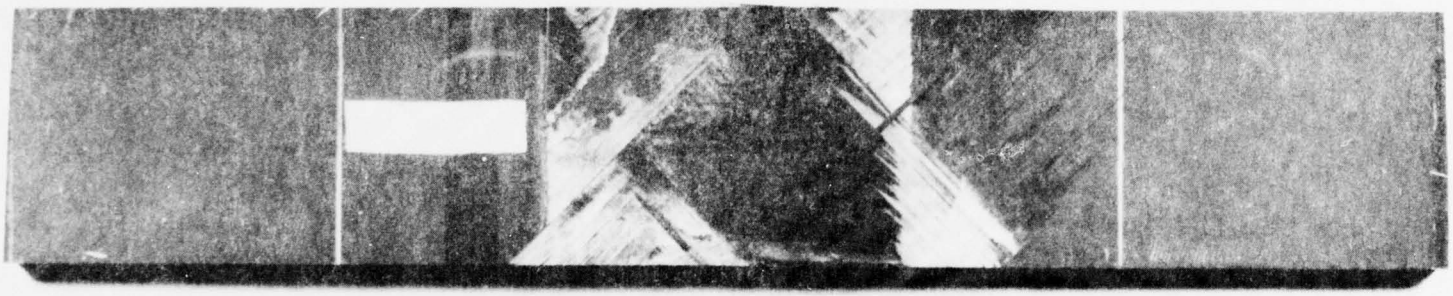

FIGURE 34. LOWER SPAR CAP PULL-OFF
TYPICAL SPECIMEN FAILURE.

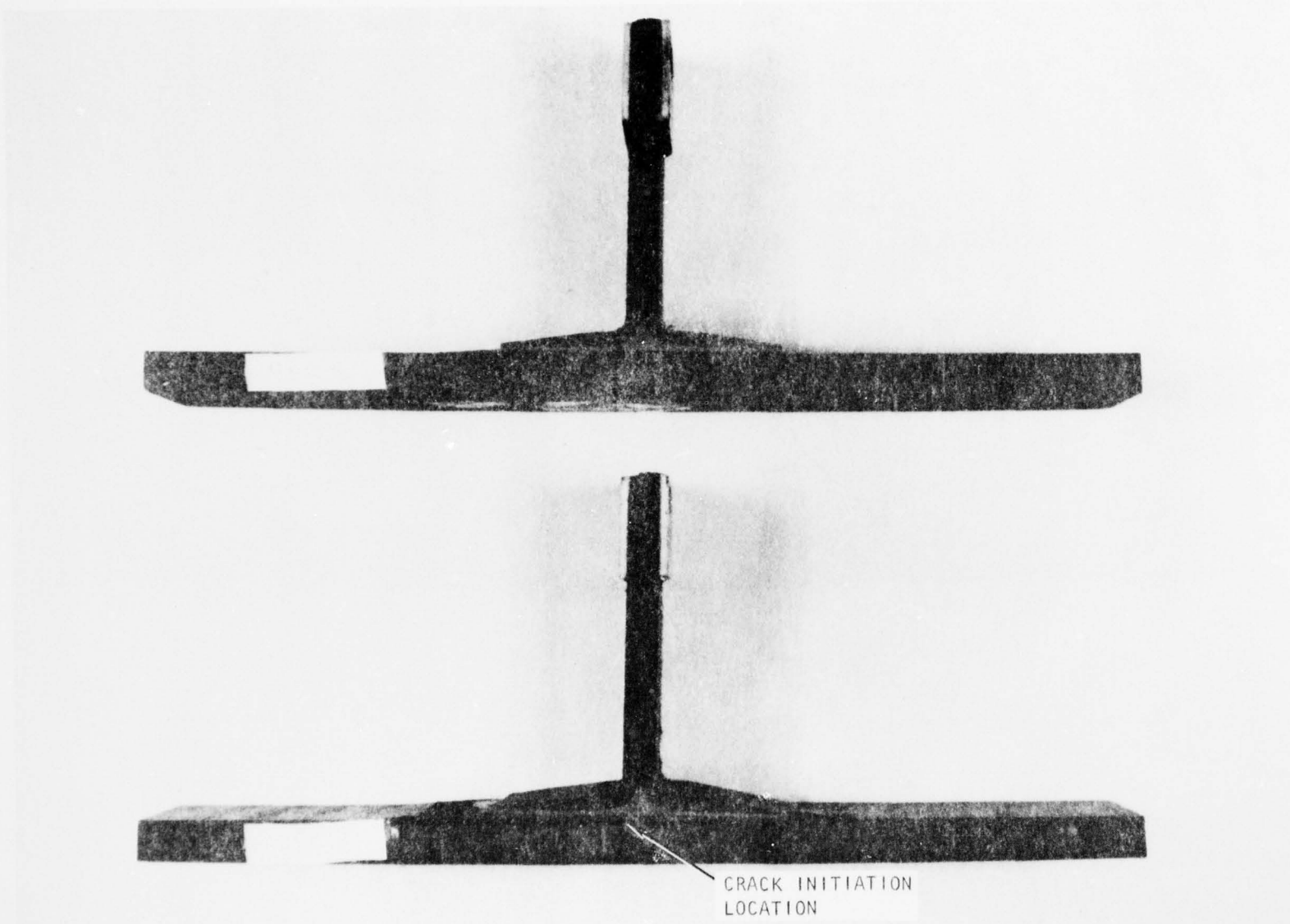

FIGURE 35. LOWER SPAR CAP PULL-OFF
FAILED SPECIMENS.

9.0 DISCUSSION AND CONCLUSIONS

Characterization of the mechanical properties of Gr/Ep composites exposed to combined temperature and humidity environments becomes possible through viscoelasticity theory and creep-recovery tests. By using the "rule of mixtures" and the Halpin-Tsai equations, a nomograph, established through a test and analysis procedure, was developed to relate shear and transverse moduli of the composite to the basic ± 45° specimen test data. This eliminates the need for obtaining biaxial creep-recovery strain data in severe environments which was not attainable in this present phase.

The test technique developed was critical to the success of this program since all the tests were scheduled to be performed in severe environments. The strain gage method was evaluated and was susceptible to moisture degradation even when the gages were coated by other resins such as M-coat C or M-coat D (Micromeasurement). Extensometers made with hermetically sealed LVDT's were found to be valid and accurate measuring devices in these severe environments. An analytical technique was formulated to correlate ± 45° specimen test data to other mechanical properties in order to fully characterize the composite. Test techniques developed in this program are very sensitive to temperature change in the test environment. From our calibration, a ± 4°F temperature differential is sufficient to introduce appreciable scatter in the test results. We were able to confine the temperature change to ± 2°F.

The effect of moisture and temperature on the mechanical response of AS/3501-6 material has been characterized through a linear viscoelastic shift factor and the creep compliance was obtained from creep-recovery test results obtained at various temperature and humidity levels. The time-scale shift factor, a function of both temperature and humidity, has a product form consisting of a temperature dependent only function and a humidity dependent only function. This product form, shown in equation (23), represents the equivalence in time-scale between the effect of temperature and the effect of humidity, since these shift factors, temperature-shift factor and humidity shift factor, are additive in the logarithmic scale. The initial compliance response is affected linearly by temperature and humidity.

In the process of characterizing composites through creep-recovery testing, two creep stress levels were used to ascertain stress dependent effects. It turned out that the lower stress level tests for both the 45° specimen and the 90° specimen have irregular creep patterns and the results were not as consistent as those run in the higher stress level tests. It is postulated that Coulomb friction in the moisture saturated specimen consumes a higher fraction of the total applied stress for lower stress level tests as compared with those of higher stress level tests. For this reason only the higher creep stress test results were analyzed.

The reduced data from creep-recovery tests also indicate that creep deformation tends to grow from one creep cycle to another creep cycle at high humidity or high temperature. As a rough estimate, Figure 36 indicates the region where temperature and humidity has an effect significant enough to create a 50 μin/in strain growth from the first creep cycle to the third creep cycle. Those data were put in a lesser weight in their application to data analysis for master curves.

As mentioned in the "Introduction" section, we had three objectives to begin with for this Phase I Research Program. On the first objective, we have shown that master curves of material properties can be characterized through the use of the viscoelastic analysis. Based on the test results, the equivalence of the thermal conditioning effect and the humidity conditioning effect on the composite materials response, the third objective has been met. They are linearly additive with regards to the initial compliance response and logarithmically additive with regards to the transient compliance response. Hence, a definite equivalence relationship between them is not feasible. The second objective on fatigue will be investigated in the next phase of the program. Additional studies which need to be done in this program are summarized below.

1. Direct biaxial measurements should be made to experimentally obtain mechanical properties and correlate them with the analysis procedure developed in the program. To conduct environmental testing by using other fiber angled specimens is an alternate approach to biaxial measurement.

2. Creep-recovery data indicate that initial creep compliance D_o tends to decrease as temperature or humidity reaches the growth region in Figure 36. It is possible that the material behavior gradually

deviated from the power law representation when it was tested at environments close to its wet glass transition temperature.

3. Our test data on D_o and n of the power law equation can be further refined if we can find another D_1 value from the recovery period in addition to that obtained from the creep period.

4. To obtain better values of graphite shear modulus, G_f, resin Poisson's ratio, ν_m, and Halpin-Tsai equation constants ζ_e and ζ_g, a new angle ply specimen, instead of ±45°, should be selected. Sensitivity results obtained by using equation (22) indicated that the ± 45° specimen results were not sensitive enough to their variations.

5. The fatigue test for the 90° specimen is very sensitive to the process of fabrication, material handling, machining, tabbing, and cutting. In essence, the 90° composite specimens should be fabricated and handled carefully to minimize the possible defect sources.

6. Assessment of the fatigue characteristics of composites in severe environments can be obtained by conducting fatigue tests on 90° and ± 45° specimens. A detailed approach to this problem will be worked and reported on in the second phase of this program.

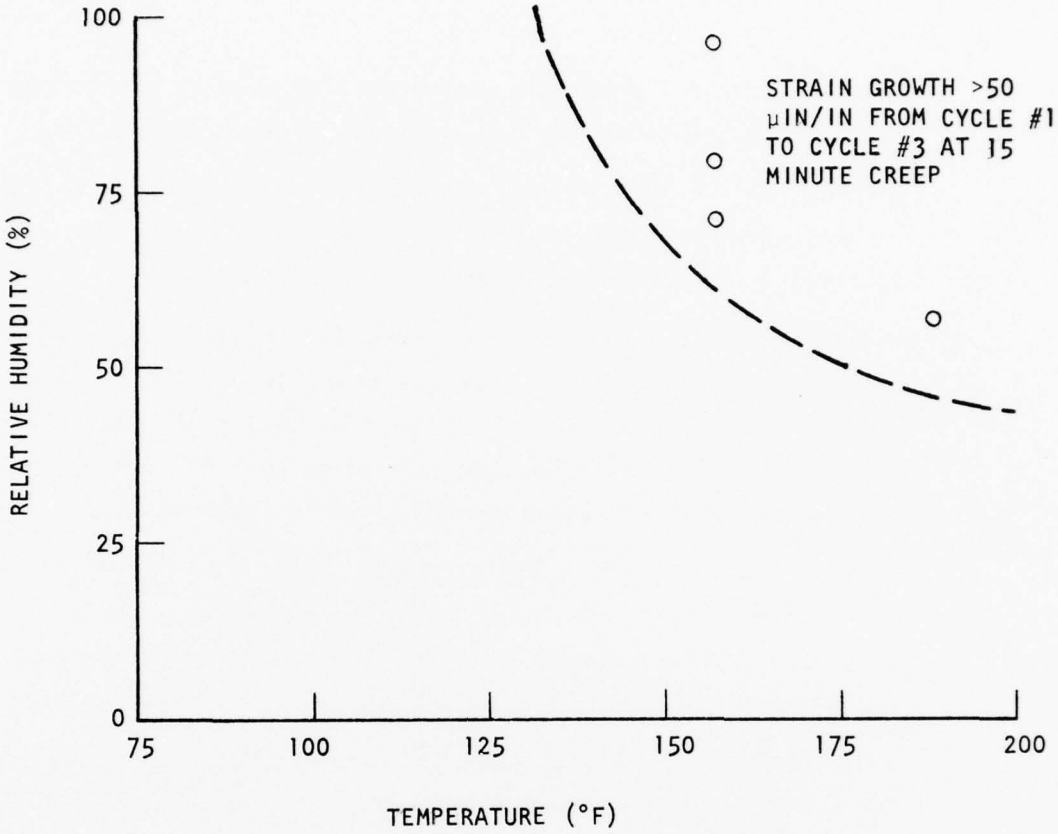

FIGURE 36. MULTIPLE-CYCLE CREEP GROWTH REGION AS CAUSED BY TEMPERATURE AND HUMIDITY.

10.0 REFERENCES

1. Shen, C. H. and Springer, G. S., "Moisture Absorption and Desorption of Composite Materials," Journal of Composite Materials, Vol. 10, January 1976, pp. 2-20.

2. Freynik, H. S. and Ditthenner, G. R., "Strain-Gage Stability Measurements for Years at 75°F in Air," Lawrence Livermore Laboratory Report.

3. Schapery, R. A., "Deformation and Failure Analysis of Viscoelastic Composite Materials," Proceedings of ASME National Meeting, Special Session on Inelastic Behavior of Composite Materials, AMD Vol. 13, December 1975.

4. Sims, D. F., "In-Plane Shear Stress-Strain Response of Unidirectional Composite Materials," Journal of Composite Materials, Vol. 7, 1973, p. 124.

5. Schapery, R. A., "Viscoelastic Behavior and Analysis of Composite Materials," in Composite Materials, Volume 2, edited by G. P. Sendeckyi, AP, 1974.

6. Browning, C. E., Husman, G. E., and Whitney, J. M., "Moisture Effects in Epoxy Matrix Composites," ASTM STP 617, 1977, pp. 481-496.

7. Lou, R. C. and Schapery, R. A., "Viscoelastic Characterization of Nonlinear Fiber-Reinforced Plastic," Journal of Composite Materials, Vol. 5, 1971, p. 208.

8. Ashton, J. E., Halpin, J. C. and Petit, P. H., "Primer on Composite Materials Analysis," Technomic Publication, 1969.

9. Garg, S. L., Svalbenas, V. and Gurtman, G. A., "Analysis of Structural Composite Materials," Marcel Dekker, 1973.

10. Schapery, R. A., Beckwith, S. W. and Conrad, N., "Studies on the Visco-Elastic Behavior of Fiber Reinforced Plastic," AFML-TR-73-179, July 1973.

11. White, D. J. and Lauridia, R. R., "Flight Spectrum Development For Fighter, Aircraft", NADC-76132-30, July 1977.

DISTRIBUTION LIST

Naval Air Systems Command
Attn: Code AIR-52032D (3)
Code AIR-950D6 (12)
Code 320A (3)
Washington, D. C. 20361

Office of Naval Research
(Code 472)
Washington, D. C. 20350

Office of Naval Research, Boston
495 Summer St.
Boston, MA 02210
Attn: Dr. L. H. Pebbles

Naval Research Laboratory
Codes 6306, 6120, 8433
Washington, D. C. 20350

Naval Ordnance Laboratory
Code 234
White Oak, Silver Spring, MD 20910

Air Force Materials Laboratory
Wright-Patterson AFB, Ohio 45433
Attn: Codes LC 1
LN 1
LTF 1
LAE 1

Air Force Flight Dynamics Laboratory
Wright-Patterson AFB, Ohio 45433
Attn: Code FDTC

Defense Ceramic Information Center
Battelle Memorial Institute
505 King Ave.
Columbus, Ohio 43201

Illinois Institute of Technology
Research Institute
10 West 35th Street
Chicago IL 60616
Attn: Dr. K. Hofer

Brunswick Corporation
Technical Products Division
325 Brunswick Lane
Marion, VA 24354

Director
Plastics Technical Evaluation Center
Picatinny Arsenal
Dover, NJ 07801

Grumman Aerospace Corp.
Bethpage, NY 11714
ATTN: Mr. G. Lubkin

HITCO
1600 W. 135th St.
Gardena, VA 90406

AVCO Corporation
Applied Technology Division
Lowell, MA 01851

Department of the Army
Army Materials & Mechanics Research
Center
Watertown, MA 02172

North American Aviation
Columbus Division
4300 E. Fifth Ave.
Columbus, Ohio 43216

Rockwell International Corp.
12214 Lakewood Blvd.
Downey, CA 90241
ATTN: Mr. C. R. Rousseau

McDonnell-Douglas Corporation
Douglas Aircraft Company
3855 Lakewood Blvd.
Long Beach, CA 90801
ATTN: Mr. R. J. Palmer

General Electric Company
Valley Forge Space Center
Philadelphia, PA 19101

Monsanto Research Corporation
1515 Nicholas Road
Dayton, Ohio 45407

Material Sciences Corporation
1777 Walton Road
Blue Bell, PA 19422

DISTRIBUTION LIST
(Continued)

U. S. Army Air Mobility R&D Laboratory
Fort Eustis, VA 23607
ATTN: SAVDL-EU-SS (Mr. J. Robinson)

B. F. Goodrich Aerospace & Defense
Products
500 South Main St.
Akron, Ohio 44318

Great Lakes Research Corporation
P. O. Box 1031
Elizabethton, TN 37643

Lockheed California Co.
Box 551
Burbank, CA 91520
ATTN: Mr. J. H. Wooley

Lockheed-Georgia, Co.
Marietta, GA 30063
ATTN: Mr. L. E. Meade

Lockheed Missiles & Space Co.
Sunnyvale, CA 94088
ATTN: Mr. H. H. Armostrong
Dept. 62-60

TRW, Inc.
23555 Euclid Ave.
Cleveland, Ohio 44117

E. I. DuPont de Nemours & Co.
Textile Fibers Dept.
Wilmington, DE 19898
ATTN: Mr. C. Zwebel

Bell Aerospace Co.
Buffalo, NY 14240
ATTN: Mr. F. M. Anthony

Union Carbide Corporation
Chemicals & Plastics
One River Road
Bound Brook, NJ 08805

General Dynamics
Convair Aerospace Division
P. O. Box 748
Ft. Worth, Texas 76101
ATTN: Tech Library

General Dynamics
Convair Division
P. O. Box 1128
San Diego, CA 92138
ATTN: Mr. W. Scheck
Dept. 572-10

TRW, Inc.
Systems Group
One Space Park, Bldg. 01
Redondo Beach, CA 90278

McDonnell Douglas Corp.
McDonnell Aircraft Co.
P. O. Box 516
St. Louis, MO 63166
ATTN: Mr. R. Jugens

Fibers Materials Inc.
Biddeford Industrial Park
Biddeford, ME 04005
ATTN: Mr. J. Herrick

General Electric
R&D Center
Box 8
Schnectady, NY 12301
ATTN: Mr. W. Hillig

Stanford Research Institute
333 Ravenswood Ave.
Bldg. 102B,
Marlo Park, CA 94025
ATTN: Mr. M. Maximovich

North American Aviation
Columbus Division
4300 E. Fifth Ave.
Columbus, Ohio 43216

University of California
Lawrence Livermore Laboratory
P. O. Box 808
Livermore, CA 94550
ATTN: Mr. T. T. Chiao

Hercules Incorporated
Magua, UT 84044
ATTN: Mr. E. G. Crossland

DISTRIBUTION LIST
(Continued)

Northrop Corporation
3901 W. Broadway
Hawthorne, CA 90250
ATTN: R. L. Jones;
Dept. 3870-62

Pratt & Whitney R&D Center
United Aircraft Corp.
W. Palm Beach, FL 33402
ATTN: Dr. J. Winfree

Naval Air Propulsion Test Center
Trenton, NJ 08628
ATTN: Mr. J. Glatz

Commander
U. S. Naval Weapons Center
China Lake, CA 92555

Celanese Research Company
Box 1000
Summit, NJ 07901
ATTN: Mr. R. J. Leal

Naval Ship Engineering Center
Code 6101E
Navy Dept.
Washington, D. C. 20360

NASA Headquarters
Code RV-2 (Mr. N. Mayer)
600 Independence Ave., S. W.
Washington, D. C. 20546

The Boeing Company
Aerospace Division
P. O. Box 3707
Seattle, WA 98124

Boeing-Vertol Co.
P. O. Box 16858
Philadelphia, PA 19142
ATTN: Dept. 1951

Commander
Naval Air Development Center
Warminster, PA 18974
ATTN: Aero Materials Lab
Aero Structures Div.
Radomes Section

Westinghouse R&D Center
1310 Beulah Rd.
Churchill Boro
Pittsburgh, PA 15235
ATTN: Mr. Z. Sanjana

Naval Ship R&D Center
Annapolis, MD 21412
ATTN: Mr. M. Krenzke, Code 727

NASA
Langley Research Center
Hampton, VA 23665

United Aircraft Corporation
United Aircraft Research Laboratories
East Hartford, CT 06108

United Aircraft Corporation
Pratt & Whitney Aircraft Division
East Hartford, CT 06108

United Aircraft Corporation
Hamilton-Standard Division
Windsor Locks, CT 06096
ATTN: Mr. T. Zajac

United Aircraft Corporation
Sikorsky Aircraft Division
Stratford, CT 06602
ATTN: Mr. J. Ray

Union Carbide Corporation
Carbon Products Division
P. O. Box 6116
Cleveland, OH 44101

Philco-Ford Corporation
Aeronutronic Division
Ford Road
Newport Beach, CA 92663

University of Maryland
College Park, MD 20742
ATTN: Dr. W. J. Bailey

University of Wyoming
Mechanical Engineering Dept.
Laramie, WY 82071
ATTN: Dr. D. F. Adams